TÉCNICO LISBOA

Manipulations of striatal temperature cause dose dependent changes in duration judgments

Ana Margarida Pexirra Tomé

Thesis to obtain the Master of Science Degree in

Biomedical Engineering

Supervisor: Prof. Dr. Joseph James Paton
Co-Supervisor: Prof. Dr. Patrícia Margarida Piedade Figueiredo

Examination Committee

Chairperson: Prof. Dr. Luís Humberto Viseu Melo
Supervisor: Prof. Dr. Joseph James Paton
Member of the Committee: Prof. Dr. Michael A. Long

November 2018

”Time is nature’s way to keep everything from happening all at once.”

Acknowledgments

I have heard before that the best things happen when you least expect it and the last six months are undeniable proof of this saying. The opportunity of doing my dissertation project in neuroscience at the learning laboratory of Champalimaud Centre for the Unknown could not have been a better start to what I am hoping to be a life dedicated to the study of the brain.

Firstly, I would like to thank Joe Paton for this amazing chance and for all his guidance, support and contagious every-day excitement about doing great science. I am also extremely grateful to all my lab colleagues for providing me with such a laid-back yet exceptionally enriching and enthusiastic environment to work. Particularly, I would like to thank (A LOT!) Tiago and Filipe for all the patience, the companionship, the late pizza nights at the lab and for the constant battle against my impostor syndrome since day one. Learning and working with each one of you inspires me every day and has been an absolute honour and pleasure.

Right after my supervisor and all my colleagues, I would like to express my deep gratitude to all my loving family for the constant support and encouragement words: à minha mãe e ao meu pai pelo carinho, apoio, paciência e orgulho incondicionais. Aos meus irmãos Ana e Zeca pela boa disposição e por me animarem nos momentos mais difíceis. Aos meus tios Lurdes e Tierri por todas as palavras ternas e por serem a voz da calma e da razão. Aos meus primos Leonor, Clara e Vasco pela sua alegria contagiante. Aos meus queridos avós, aos que cá estão e aos que tanto gostariam de ainda cá estar, pelo orgulho e por todo o amor que têm por mim. A Álvaro y a su sonrisa, que es donde vive la mía.

I cannot pass on my thanks without mentioning Alan, Chandler, Joey and Roger. This project and neuroscience would not exist without you.

Finally, I want thank all my friends and university colleagues for living and sharing the joys and frustrations of these last five years with me.

This has been an amazing journey and the presence of each one of you was what made it so special and what will make me cherish it forever.

Resumo

O tempo, tal com o espaço, é uma dimensão fundamental na vida dos animais. Um comportamento adaptativo requer que os organismos extraiam do ambiente uma estrutura temporal através de experiência e construam um comportamento temporalmente padronizado. O corpo estriado é uma estrutura dos gânglios da base que recebe projecções de diversas áreas corticais e que está envolvida em funções dependentes do tempo como aprendizagem por reforço ou quantificação de intervalos de tempo numa escala de segundos. Projectos anteriores do laboratório manipularam e registaram actividade de neurónios do corpo estriado de ratos durante a realização de uma tarefa psicofísica de categorização de intervalos. Estes estudos mostraram que a dinâmica do corpo estriado traduz juízos de tempo e que a actividade de conjuntos de neurónios do corpo estriado registada em simultâneo foi capaz de determinar a duração de um intervalo tão acertadamente quanto o animal. Adicionalmente, os neurónios do corpo estriado foram necessários na determinação do intervalo de tempo tendo em conta que infusões de muscimol nesta área induziram uma dessensibilização à percepção de tempo dos animais. Finalmente, foi ainda descoberto que o tempo estava codificado na velocidade da dinâmica da população de neurónios: dinâmicas mais rápidas previram juízos de durações mais longas e vice-versa. De forma a avaliar se a variabilidade na velocidade da dinâmica da população do corpo estriado causa variabilidade no juízo de tempo, manipulámos a temperatura desta estrutura durante a realização da tarefa com um dispositivo termoeléctrico personalizado. As sessões de comportamento foram divididas em blocos de duração fixa: blocos de controlo (nos quais o dispositivo foi colocado à temperatura corporal), intercalados com blocos de manipulação (nos quais a temperatura do dispositivo alternava entre diferentes doses). Os resultados mostram que arrefecer/aquecer o tecido do corpo estriado causou subestimação/sobreestimação de tempo graduais. Notavalmente, variáveis motoras não foram afectadas pelas manipulações de temperatura. Estes dados apoiam fortemente a hipótese de que a dinâmica de populações neurais está subjacente a estimativas de tempo e que o corpo estriado dorsal é um local onde uma variável de decisão relacionada com o tempo decorrido e independente da função motora pode ser manipulada.

Palavras-chave: codificação de tempo, comportamento, corpo estriado, dinâmicas neuronais, gânglios da base, juízos de tempo, manipulação de temperatura

Abstract

Time, like space, is a fundamental dimension of animals' worlds. To behave adaptively, organisms must extract temporal structure from experience and construct temporally patterned behavior. The striatum is the main input of the basal ganglia and has been implicated in several time-dependent functions such as reinforcement learning and timing behavior. Previous work from the lab manipulated and recorded the activity of striatal neurons while rats performed an interval categorization psychophysical task. It was found that simultaneously recorded neuronal ensembles could judge time as well as the animal and that striatal neurons were necessary for duration judgments, as muscimol infusions produced a clear decrease in temporal sensitivity. Lastly, these studies showed that time was encoded in the speed of population dynamics: faster dynamics were correlated with longer duration judgments and vice-versa. To directly assess whether variability in the speed of striatal population dynamics causes variability in duration judgments, we experimentally manipulated striatal temperature during task performance using a custom-made thermoelectric device. Behavioral sessions were divided in fixed-time blocks: control blocks (in which the device was set to body temperature), interspersed with manipulation blocks (in which the temperature changed between different doses). Here we show that cooling/warming striatal tissue caused graded underestimation/overestimation of duration, respectively. Critically, motor-related variables were not affected. These data strongly support the hypothesis that dynamics in neural populations underlie duration estimation, and establish the dorsal striatum as a locus within neural circuitry where a decision variable related to elapsed time and independent of motor function may be manipulated.

Keywords: basal ganglia, behavior, duration judgments, neural dynamics, striatum, temperature manipulation, time encoding

Contents

Acknowledgments v
Resumo vii
Abstract ix
List of Figures xiii

1 Introduction **1**
1.1 Why studying time? 1
1.2 Objectives 1
1.3 Thesis Overview 2

2 State-of-the-art **3**
2.1 A Brief History of (neural) Time 3
2.2 Temperature Manipulations in Neural Studies 7
2.3 Theoretical Background 11
2.3.1 Basal Ganglia 11
2.3.2 Striatal Neurons 12
2.3.3 Peltier Effect 14
2.4 Theoretical Hypothesis 15

3 Methods **17**
3.1 Subjects 17
3.2 Experimental Setup 17
3.3 Behavior 19
3.3.1 Training Stages 19
3.3.2 Interval Categorization Task 20
3.4 Thermoelectric Cooling (TEC) Device 21
3.4.1 Design and Architecture 21
3.4.2 Temperature Control and Readout 23
3.4.3 Testing 23
3.5 Surgical Procedure 24
3.6 Manipulation Sessions 25
3.7 Data Analysis 25

3.8 Perfusion 26
3.9 Magnetic Resonance Imaging (MRI) 26

4 Results **29**
4.1 TEC Device Testing 29
4.2 Animal Training 31
4.3 Behavior in Manipulation Sessions 34
4.4 MRI 42

5 Conclusions **45**
5.1 Discussion 45
5.2 Future Work 48
5.3 Personal Remarks 49

Bibliography **51**

List of Figures

2.1 Striatal dynamics explain duration judgments . . . 6
2.2 Temperature manipulations as a method to study neural circuit dynamics . . . 9
2.3 Diagrams of the basal ganglia anatomy and its neural circuits . . . 12
2.4 Schematic of the Peltier effect . . . 14
2.5 Data simulation of the theoretical hypothesis . . . 15

3.1 Experimental setup and main components of a nose port. . . . 18
3.2 Interval categorization task. . . . 20
3.3 Implant architecture. . . . 22
3.4 Coronal view of the implant targeting the dorsal-central striatum. . . . 24
3.5 Psychometric functions provide readily interpretable quantities that summarize behavior in 2AFC tasks . . . 26

4.1 Transfer function between set temperatures and measured temperatures at the lower plate and probe's tips. . . . 30
4.2 Example session from training stage 2. . . . 32
4.3 Performance evolution in the interval categorization task. . . . 32
4.4 Animals progressed similarly across the various stages in our tranining protocol. . . . 33
4.5 Animals showed a consistent behavior performing the interval categorization task before and after the surgeries. . . . 33
4.6 Discrimination behavior of individual animals across all manipulation sessions. . . . 35
4.7 Temperature manipulations caused dose-dependent changes in duration judgments. . . . 35
4.8 Manipulation effect on behavior changed from the first to the last manipulation session. . 37
4.9 Magnitude of the temperature effect size progressively dwindled across sessions. . . . 38
4.10 Magnitude of manipulation effects is nonstationary within blocks. . . . 39
4.11 Changes in striatal temperature caused bidirectional and graded changes in estimates of elapsed time. . . . 41
4.12 Animals' motor responses were not affected by changes in the striatal temperature. . . . 42
4.13 Implant probes were successfully placed in the dorsal-central striatum of all three animals 43

Chapter 1

Introduction

1.1 Why studying time?

Time, like space, is a fundamental and consistently present dimension in the environment and, more broadly, in life.

If one considers the ability of interacting with the external world a crucial condition of being alive, the importance of timing for living beings becomes evident. Interactions of organisms with their surrounding environment are characterized by a coordinated execution of intricate behaviors with a remarkable and contextualized temporal precision. From more animal behaviors such as foraging for food or courtship for selecting partners for reproduction to more human facets of behavior such as speaking, dancing or writing a master thesis within a stipulated deadline, all of these behaviors are executed in temporally coordinated sequences.

The nervous system evolved to allow animals to adapt to and anticipate events in a dynamic world (Merchant, 2014), making timing critical to most forms of learning behavior and sensory-motor processing (Paton and Buonomano, 2018).

Despite performing temporally ordered sequences being irrevocably one of the most outstanding and essential brain functions, there is no evidence of a specific biological system or ”time brain area” that senses and processes time as there is for sight, hearing or taste (Merchant et al., 2013).

Timing is everything. Nevertheless, the way temporal information is represented and processed in the brain is still poorly understood, thus the urgency of studying time’s neural basis and its underlying mechanisms.

1.2 Objectives

The main purpose of this project is to corroborate previous results providing strong evidence that the dynamics of striatal neurons can predict duration judgments. Hereby, we are trying to collect evidence of a causal relation between the speed of striatal population dynamics and the animal’s judgment of the elapsed time while performing an interval categorization task.

To accomplish such results, the main landmarks to be achieved along this project are:

1. Design, characterize and validate custom-made thermoelectric implants.
2. Train rats to perform an interval categorization psychophysical task.
3. Surgically implant the custom-made thermoelectric device developed in dorsal-central striatum.
4. Manipulate the temperature of striatal tissue during behavioral sessions.
5. Analyse the collected data during the manipulation sessions using MATLAB.

1.3 Thesis Overview

The work presented in this monograph is organized into five different chapters.

This first chapter intends to generally introduce the problem and contextualize the study we did for the past semester, starting by highlighting the relevance of studying timing in biological systems and in adaptive behavior and ending with this outline, after stating the main goals we intend to achieve with this project.

In chapter 2, we made a bibliographic review including relevant literature for discussing work presented in the following chapters. Particularly, this review includes insights on theoretical and experimental research done so far in time estimation and the basis of its neural mechanisms. Further into this chapter, the advantage of using temperature as systematic method to study neural physiology instead of other commonly used methods such as lesion or drugs is discussed. For this purpose, we describe the results found by several research groups relative to temperature manipulations in the nervous system, both from a more molecular and biophysic point of view to studies inserted in a more behavioral context. After summarizing the crucial state-of-the art necessary to understand our work, we felt the need to clarify the theoretical background of some key concepts frequently discussed throughout this thesis. This chapter ends with the presentation of our theoretical hypothesis and our expectations for the results.

Chapter 3 was included with the purpose of describing the methods, materials and procedures used along this project. By dividing this chapter into different sections, we provide the reader a clearer idea of the main tasks that had to be developed throughout this project as well as some sense of the time allocated to each assignment.

In chapter 4 we present the results of our project in a chronological way, starting with the results of the development and engineering of the used brain implant. Following the characterization of the brain implant, results regarding animal training and performance in the task are shown. This chapter ends with the results of animals' behavior in the sessions where striatal temperature was manipulated.

Finally, chapter 5 consists of an overall discussion of the work presented, where we summarize and contextualize our findings. Additionally, we discuss future studies that can be done to enlighten some of the work developed that is not yet fully understood. Lastly, I leave the reader with some final remarks about the importance and the contribution of this last semester to my personal growth as a biomedical engineer and, most importantly, as a future scientist.

Chapter 2

State-of-the-art

2.1 A Brief History of (neural) Time

Time is essential for almost all forms of learning, behavior and daily life activities such as moving or communicating with others.

The ability of interacting with the environment relies on the evolutionary development of adaptive systems that are able to capture the variation of events in the environment across time. By being adaptive, these systems learn to produce a specific behavior at a specific time, in order to achieve the planned and desired outcome. These variations in the environment and consequent adaptive response of an organism can happen at different time scales (Buonomano, 2007). From circadian rhythms, which are a biological timing system that organizes the environmental oscillations every 24 h (Merchant, 2014), to representations of time in the order of the microsecond to millisecond, a range implicated in transcription-translation autoregulatory feedback loops, now it is known that the brain uses distinct mechanisms to tell time according to the time scale (Paton and Buonomano, 2018).

Although animals are able to represent such a large dynamic range of timescales, the most critical one on most forms of learning and behavior lies in the scale of seconds to minutes (Paton and Buonomano, 2018). The quantification of intervals in this seconds to minutes range is referred by many authors as interval timing and it is involved, amongst others, in foraging, decision making and coordinated motor responses (Buhusi and Meck, 2005). Furthermore, at this scale there is an influence of other cognitive processes such as attention and memory, which interact with the mechanisms of quantification of intervals in this range of time (Hinton and Meck, 1997; Meck and Ivry, 2016).

Some research areas in neuroscience are interested in understanding the mechanisms of timing in the brain during interval timing. These studies can be carried out using a broad repertoire of different methods that are commonly distinguished into four distinct classes of behavioral protocols (Grondin, 2010):

> **Verbal estimation:** subjects are presented with a stimulus, then required to give a estimation of its duration, using chronometric units. Due to the necessity of a verbal answer, these type of tasks are restricted to human participants, conditioning the study in other animal models.

Reproduction: subjects are presented with a stimulus and are asked to reproduce the length of the presented interval by means of some operation.

Production: subjects are asked to produce a temporal interval specified by the experimenter, without being previously exposed to the stimulus.

Method of comparison or interval/duration discrimination: subjects are asked to discriminate which relative duration of two presented intervals/durations is the longest/shortest, or to make a judgment as whether a presented interval/duration is longer or shorter than a standard one.

The task we use in our study is a variant of the method of comparison, called the single-stimulus method. In a single-stimulus method, instead of a direct comparison between two stimuli, the subjects judge a presented interval by assigning it to one of two categories: short or long (Grondin, 2010), where only one of the two choices is reinforced. By being forced to discriminate stimuli into two classes, these paradigms are commonly referred in the literature as two-alternative forced-choice (2AFC) tasks. 2AFC paradigms are a widely used approach in psychophysics for measuring sensory thresholds, thus quantifying the sensitivity of a specific sensory system (Ulrich and Miller, 2004; Carandini and Churchland, 2013; Gold and Shadlen, 2007). The results given by these kind of tasks can be graphically visualized as a psychometric function, in which the probability of categorizing a stimulus into a particular class is plotted as a function of the stimulus strength (Lapid et al., 2008). Typically, when the y-axis denotes the probability of categorizing a given stimulus duration as long, this curve assumes values near 0 at small stimuli values and approaches 1 for large stimuli values. By fitting a psychometric curve to these data, it is possible to estimate the point of indifference of a subject to that particular stimulus, i.e. the interval that a subject is equally likely to judge as long or short (Wichmann and Hill, 2001). The steeper the fitted psychometric function is, the higher is the differential sensitivity of the observer to the stimulus being studied (Lapid et al., 2008).

Despite all effort done so far in the development of different behavioral paradigms as well as several computational models, the mechanisms underlying timing on the scale of milliseconds and seconds are still poorly understood. From a broad point of view, these models can be categorized into two different classes: dedicated and intrinsic models (Ivry and Schlerf, 2008). On one had, dedicated models suggest that there is some sort of specialized mechanism, associated with particular neural structures, that represents the temporal relationships between events. On the other hand, intrinsic models, which have been more and more supported with recent data, consider that there is no specialized brain system representing timing, proposing that time is inherent in neural dynamics of most neural circuits (Ivry and Schlerf, 2008). Although intrinsic models support a perspective where most neural circuits have the capacity to tell time, it is still considered that different circuits are more or less likely to be specialized to tell time (Merchant, 2014), as there are areas more involved in tasks that are inherently temporal in nature (Paton and Buonomano, 2018).

Another categorization of the several theoretical models that have been proposed to analyse the neural basis of timing can be based on the used computational strategies (Mauk and Buonomano, 2004; Paton and Buonomano, 2018).

One of the oldest and most popular views on interval timing in animals is explained by oscillator-based or pacemaker-accumulator models. The overall concept of these models relies on the existence of both a pacemaker and an accumulator structure. The pacemaker periodically generates events that are counted by an accumulator and the number of pulses counted is a measurement of the elapsed time. The most frequently cited model derived from this pacemaker-accumulator perspective is the scalar expectancy theory (Gibbon, 1977), which considers the behavioral response to result from a comparison between the current time estimation (stored in the accumulator) and a sample from the distribution of previously estimated durations (stored in reference memory as the number of pulses in the accumulator by the time of reward). Moreover, this model also considers that the variability of time judgments is linearly proportional to the mean representation of time. Other oscillator-based models have been proposed over the years (Matell and Meck, 2000), such as the Behavioral Theory of Timing (Killeen and Fetterman, 1988), the Learning to Time (Machado, 1997) or more recently the Striatal Beat Frequency model (Matell and Meck, 2004).

A different view proposing that time is encoded in the changes of neural activity of a population is hypothesized by state-dependent models, also referred as population clocks. A population clock can be defined as a neural trajectory in a space which dimension is defined by the number of neurons that constitute the clock. Taking this definition into account, each point on the trajectory is responsible for coding for a moment in time. Therefore, if these patterns can be reproduced and are unique at each moment, downstream neurons are able to readout elapsed time (Paton and Buonomano, 2018). The most representative example of this no-dedicated-system view is the one referred to as a state-dependent network (SDN) (Grondin, 2010). SDN models propose that for spans on the scale of tens to hundreds of milliseconds, time may be represented as specific states of a neural network, meaning that timing does not depend on a clock, but rather on time-dependent changes in the state of neural networks (Buonomano and Karmarkar, 2002).

All these and other non-mentioned theories try to model and reproduce several aspects of timing behavior in many interval timing tasks but neural data in conflict or in support of the various theories are still lacking.

Ultimately, the most fundamental step in understanding the neural basis of temporal processing is to find neurons that are selective to the temporal features of sensory stimuli or responsible for the generation of timed motor responses (Mauk and Buonomano, 2004).

Several studies over the past years have been able to identify timing related signals in the neural activity in multiple brain areas such as the hippocampus (MacDonald et al., 2011; Pastalkova et al., 2008), cerebellum (Braitenberg, 1967; Ivry and Keele, 1989; Mauk and Buonomano, 2004), medial prefrontal (Kim et al., 2013; Xu et al., 2014), motor (Mita et al., 2009) and parietal (Janssen and Shadlen, 2005; Leon and Shadlen, 2003) cortices and the basal ganglia (Jin et al., 2009; Mello et al., 2015; Gouvêa et al., 2015) (for a more detailed and comprehensive review on these studies see Mauk and Buonomano (2004); Grondin (2010); Coull et al. (2011); Paton and Buonomano (2018)).

One important study that shows evidence that the basal ganglia, more specifically the striatum, is involved in the representation of sensory timing was done by our lab, being the main motivation for this

dissertation (Gouvêa et al., 2015). Gouvêa and colleges found that striatal dynamics are necessary for and are able to explain interval timing behavior in a 2AFC task, in which animals had to categorize intervals as longer or shorter than a 1.5-s categorical boundary, by making leftward/rightward movements, respectively. By simultaneously recording ensembles of striatal neurons while rats were performing the task it was observed that these neurons presented different firing patterns at different times during the interval period and the choices could be predicted using the neural activity collected during interval stimuli presentation (figure 2.1, left).

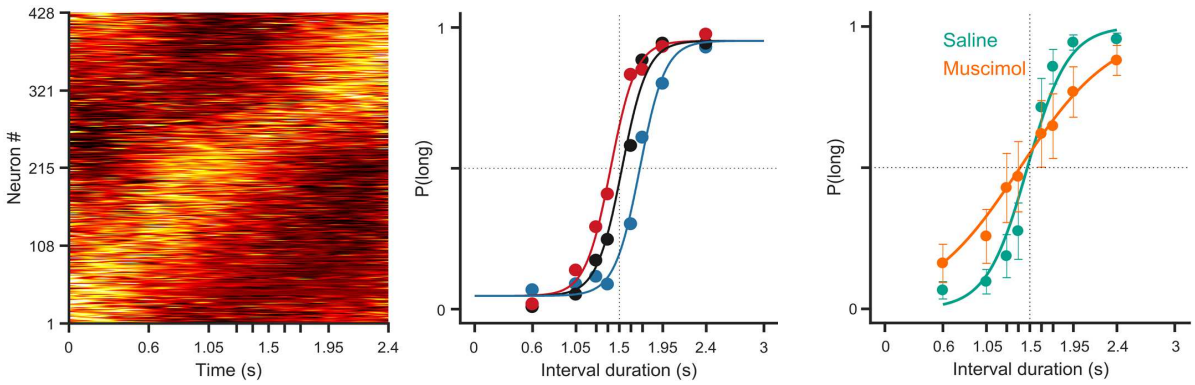

Figure 2.1: Striatal dynamics explain duration judgments. Normalized peristimulus time histograms (PSTHs) of all neurons for correct trials in which the longest stimulus interval was presented. Lighter colors represent higher normalized (z-scored) activity **(left)**. Psychometric curves constructed from trials separated according to whether the population state at stimulus offset had advanced more or less along the mean trajectory. Blue, black and red indicate the 1st, 2nd and 3rd terciles, respectively **(middle)**. Averaged psychometric curves following bilateral muscimol vs saline injections in dorsal striatum **(right)** - Adapted from Gouvêa et al. (2015).

Furthermore, the authors defined a mean trajectory in a high dimensional neural space of neural activity within each session and projected the state of simultaneously recorded neuronal populations on individual trials onto that mean trajectory. These analysis showed evidence that if a population state at stimulus offset was leading or lagging the defined mean trajectory, animals were more likely to judge near-boundary stimuli as long or short, respectively (figure 2.1, middle). These results strongly suggest that striatal dynamics encode the timing information that rats were using to guide their judgments.

Finally, to further show that striatal activity was directly involved in supporting the interval categorization task, the GABAa (γ-aminobutyric acid) receptor agonist muscimol was bilaterally injected into the rats' dorsal-central striatum. This resulted in a significant drop in the sensitivity of animals' judgment when compared to interleaved sessions in which saline was injected in the same site (figure 2.1, right), suggesting that duration categorization in this task was dependent on a normally functioning striatum and that the neural activity previously recorded was directly supporting duration judgments. However, the use of pharmacological agents such as muscimol infusions that promote neural inactivation could be compromising other important neural functions involved in task performance such as reward processing or memory for the mapping between time and choice. Therefore, a more subtle manipulation that induces changes in the speed of neuronal and circuit dynamics rather than inactivation would be more appropriate in providing stronger evidence of the role of the striatum in the control of timing.

To overcome this technical problem, this dissertation project, like the following section, intends to show that the use of precise temperature manipulations can be an elegant method to dissect neural circuits and gain further insight into their function (Robertson and Money, 2012).

2.2 Temperature Manipulations in Neural Studies

The study of a neural circuit that generates and controls temporal sequences of behaviors, even if confined to a well defined and characterized anatomical brain region, is not trivial.

To be able to test hypothesis about the physiology and dynamics of these circuits, appropriate techniques must be selected not only according to the anatomy of the problem but also, and most importantly, to the questions one wants to answer. Consequently, the selection of the appropriate techniques and methods will be crucial to a better understanding of the circuit biophysical dynamics that allow one state of the system to transform into the next state in time.

Early in neuroscience, studies in patients with brain lesions allowed neuroscientists to understand and correlate specific behavioral patterns with the location of the lesions. A familiar example of lesion studies happened over one century ago, when patients' lesions in the areas now know as Broca's (Broca, 1865) and Wernicke's (Wernicke, 1874) areas were studied by these neuroscientists, allowing them to establish a causal relationship between these delimited brain areas and the speech and language deficits observed in their patients (Damasio, 1994).

Similarly to lesion studies, pharmacological studies in which a drug induces the total inactivation of a target brain area can give us information whether a brain region is necessary for the expression of a particular behavior (Aronov and Fee, 2011). Other techniques such as electrophysiological recordings or fiber photometry can tell us if the neural activity of a brain area can disrupt or elicit a behavior. However, none of the above-mentioned strategies are able to reveal whether the biophysical dynamics within a region are actively involved in timing a behavior (Fee and Long, 2011).

Taking into account that most biological processes are highly temperature dependant, including the functioning of nerve cells (Volgushev et al., 2000b; Robertson and Money, 2012), localized temperature manipulation such as mild cooling or heating alter the speed of neuronal and circuit dynamics (Aronov and Fee, 2011).

Therefore, by inducing perturbations in the speed of neural dynamics, temperature manipulations in brain tissue allow researchers to test hypotheses about the dynamical origin of temporal structure in neural circuits, revealing the role of the manipulated area in the control of timing (Fee and Long, 2011).

A while ago, temperature manipulations were a widely used method for the study of neural circuits by doing a reversible and local activation/inactivation of neural tissue (Payne et al., 1996). However, with the increasing interest of neuroscience in understanding the interaction between different brain areas and between neural circuits and behavior, the advent of new techniques with higher spatial and temporal resolutions such as optogenetics (Fenno et al., 2011) has been substituting the use of temperature manipulations as a method to dissect neural circuits.

Before inferring any major relationship between a brain region manipulated with a temperature dif-

ferent than physiologic and a specific behavior, it is important to understand and characterize the microscopic effects induced by temperature changes at a cellular level.

Volgushev and colleges described and quantified a wide range of passive and active membrane properties and spike generation in slices from the visual cortex of rats and cats and analysed the mechanisms underlying their temperature dependence (Volgushev et al., 2000a,b). By systematic and reversible changes in the temperature of the brain slices, they observed that basic properties of neurons such as the membrane potential, the input resistance, the shape and the amplitude of action potentials and the propagation of spikes was altered. Lowering the temperature of the slices induced a marked depolarization of the cell membrane and an increase in the input resistance of the cells. By analysing the temperature dependence of the conductance of two main ionic channels contributing to the resting membrane potential (sodium and potassium), this study saw that the partial K^+ conductance had a positive correlation with temperature, unlike partial Na^+ conductance, which was essentially independent of temperature. Therefore, the total changes of membrane conductance with temperature were mostly associated to changes in the partial K^+ conductance (Volgushev et al., 2000b).

Further in these studies, temperature dependence of active membrane properties was also quantified. Mild temperature cooling reshaped the action potentials, widening their shape and increasing their amplitude from the spike origin to its peak. Furthermore, a decrease in temperature induced a decrease of the number of spikes, with a marked reduction of amplitude of the second spike and an increase in the time of the inter-spike interval. Synaptic responses were also affected by decreasing temperature of the neural tissue, inducing an increase of the latency of synaptic responses and a decrease of the amplitude of excitatory postsynaptic potentials (EPSP) (Volgushev et al., 2000a).

A decrease of spontaneous activity (spikes/second) and an increase of spike duration and width during cooling was also registered by Girardin and Martin in the neurons from the visual cortex of anaesthetized cats, with a recovery of the original values upon rewarming (figure 2.2 C) (Girardin and Martin, 2009).

At a neural population level, remarkable work on the influence of temperature in the activity of neural circuits has been done by Tang et al. with the description of temperature effects on the pyloric rhythm of the stomatogastric ganglion of crabs (Tang et al., 2010). This rhythm ensures the chewing and filtering of food in marine crustaceans and it is characterized by a triphasic motor pattern in which the lateral pyloric and pyloric neurons fire on rebound from inhibition by pacemaker neurons (anterior burster and pyloric dilator). By quantifying the pyloric network output at different temperatures, the authors observed that pyloric frequency increased significantly with temperature (figure 2.2 B). Despite this strong correlation, the phase of firing of the pyloric neurons, defined as the delay of each firing event divided by the cycle period, seemed to be unaltered by temperature changes. This suggests an increase in the activity of this neural circuit with temperature while leaving the circuit properly functioning by a maintenance of the phases at which neurons burst.

These studies support the use of temperature as a useful manipulation strategy to investigate the role of specific circuits in timing of a behavior. Because it affects many neuronal processes such as synaptic transmission and spiking properties, temperature change can be used very generally, even

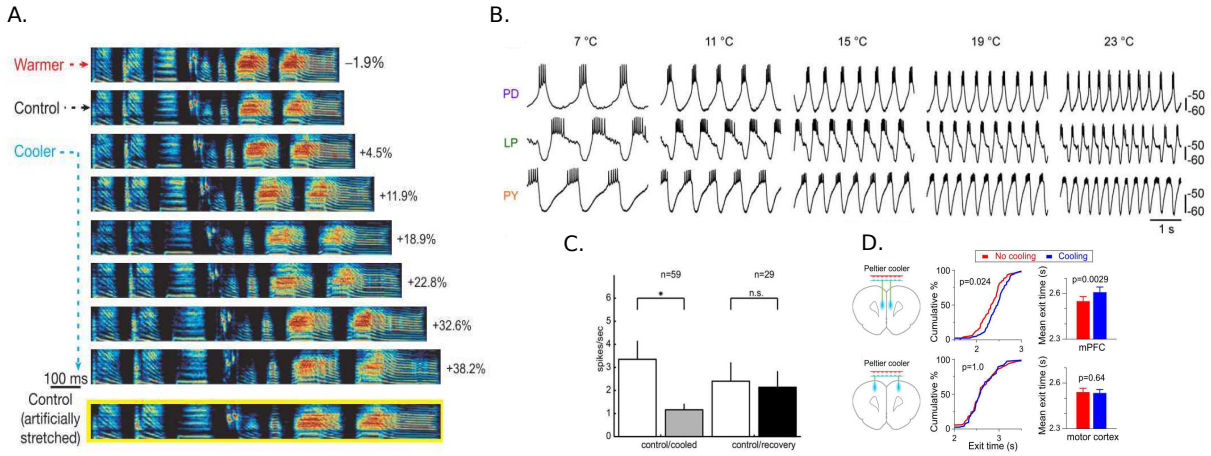

Figure 2.2: Temperature manipulations as a method to study neural circuit dynamics. (A) Representative sonograms recorded from a zebra finch with the high vocal center (HV) heated and cooled, showing percentage song dilation relative to control - Adapted from Long and Fee (2008). **(B)** Simultaneous intracellular recordings of neurons from different structures involved in the pyloric rhythm of a crab at different temperatures - Adapted from Tang et al. (2010). **(C)** Effect of cooling on the spontaneous response of single cells from a cat's visual cortex, with mean spontaneous activity during control (white), cooling (grey) and recovery (black) - Adapted from Girardin and Martin (2009). **(D)** Local cooling of medial prefrontal cortex (mPFC) delays exit times in rats performing a in a time reproduction task (top). Cooling motor cortices had no effect on exit times - Adapted from Xu et al. (2014).

without detailed knowledge of the underlying circuit or neuronal properties (Fee and Long, 2011). Despite large decreases in temperature can result in a circuit "shut-down" (Volgushev et al., 2000b; Girardin and Martin, 2009), mild cooling results in a slowing of the circuit activity, with a reversibility of the effect upon rewarming.

As for *in vivo* effects, several studies show how temperature changes in crucial structures for generating a pattern produce a significant change in the oscillatory cycle time of the neural activity, while leaving the circuit and behavioral function intact (Fee and Long, 2011).

One of the first studies to use temperature changes to localize the brain dynamics responsible for a specific behavior was done in crickets to understand the patterns of song production and recognition networks (Pires and Hoy, 1992). The authors provided experimental evidence that the speed of the crickets' song increased upon heating of their thorax. However, no changes in the speed of the song were detected when heating was only applied to the animals' head.

The model of the stomatogastric ganglion of crabs studied *in vitro* and *in silico* by Tang and colleges (Tang et al., 2010) was further studied *in vivo* (Soofi et al., 2014). These results corroborated the previous findings by again observing an increase in the *in vivo* pyloric frequency elicited by increasing temperature, while pyloric phases were generally conserved.

In rats trained to estimate time intervals by exiting a waiting port at different times according to a sound offset, temperature manipulations in the medial prefrontal cortex (mPFC) were used to directly test a causal role of the mPFC neuronal activity in the rat's time-estimation behavior. It was found that temporal scaling of mPFC neural activity was strongly correlated with the rat's time-estimation behavior during the two-interval time-estimation task, as cooling the mPFC resulted in increased exit times (Xu et al., 2014). Furthermore, in this study the cooling effect on exit times was not shown not to be due to

a general slowing of rat' movements, since there were not significant changes in the time for the rat to move from the waiting port to the reward port while cooling the motor cortex (figure 2.2 D).

Studies in song birds have provided some of the clearest evidence that population clocks in the form of sequential activation of neurons underlie some forms of motor timing (Paton and Buonomano, 2018). The songs of zebra finches have a very precise and hierarchically organized temporal structure mediated by a number of distinct motor nuclei, known as the song motor pathway (Fee and Long, 2011). Particularly, the population of neurons in two forebrain nuclei have been implicated in the control of the temporal structure of a song: the high vocal center (HVC) and the robust nucleus of the arcopallium (RA), where the first projects to the latter. Long and Fee have shown that cooling down the HVC uniformly slows the speed of the bird's song, as it was registered an increase in motif duration during cooling (figure 2.2 A) (Long and Fee, 2008). However, temperature manipulations in the RA did not result in significant changes on the song timing (Long and Fee, 2008). Moreover, the authors also measured the spiking frequency of single units in the RA in an anaesthetized preparation at different temperatures, registering a rapid linear decrease in RA neuron tonic spiking rate upon cooling of this area, hence a slowing of neural activity by means of temperature changes. Therefore, by using temperature manipulations, this study shows a causal link between the neural dynamics generated within a circuit and the timing of a motor behavior (Paton and Buonomano, 2018).

Although focal temperature manipulations are rarely performed in humans, recently, Long and colleges focally lowered the temperature of distinct cortical regions in awake neurosurgical patients to localize speech-related cortical sites (Long et al., 2016). In this study, the authors found that cooling-related effects are primarily confined to the left hemisphere. Moreover, it was noticed that cooling the speech motor cortex leads to changes in the quality of vocalizations and that cooling Broca's area often led to changes in the speech rate. Together, these results show evidence of a functional dissociation by altering speech timing and quality when cooling Broca's region and the speech motor cortex, respectively.

To some extent, all studies using temperature manipulations in the brain require a well defined engineering approach to guarantee an informed and controlled use of this manipulation variable. Thermoelectric devices based on the physical principles of the Peltier effect (see subsection 2.3.3) have been used to induce temperature changes in the brain tissue in several studies (Long and Fee, 2008; Long et al., 2016; Xu et al., 2014). For a better understanding on the main variables that one needs to take into account when using a thermoelectric device to manipulate temperature in the brain, Aronov and Fee presented a theoretical analysis of these devices and a procedure for optimizing their design, according to the needs of a specific study (Aronov and Fee, 2011). By mathematically defining the basic thermal and electrical properties of a thermoelectric device as well as simulating the spatial extent of thermal propagation in the brain, this study provides a systematic comprehension on the temperature effects for structures both deep or at the surface of the brain.

In conclusion, this section intended to motivate the use of temperature manipulations as an effective and reliable method to study neural circuit dynamics that are involved in the control of timing of a behavior, across different animal models and even in humans.

2.3 Theoretical Background

Although the reading of this section is not absolutely crucial to fully understand the developed work, it gives the reader more detailed and descriptive insights on some concepts frequently mentioned and implied along the following sections. I hope it can help the reader to understand the major anatomical, physiological and physical principles underlying these concepts as much as it helped me at the beginning of the project.

2.3.1 Basal Ganglia

The basal ganglia (BG) are a large subcortical structure composed by interconnected nuclei located in the forebrain, midbrain, and diencephalon. Literature often reports the crucial participation of the BG in the control of movement, as a large portion of its connections are with brain motor areas. Additionally to their role in motor control, BG are also involved in decision-making, action selection, reinforcement learning and cognitive and affective functions (Squire et al., 2008). Despite some anatomical differences across species, the ganglia circuitry is present in the phylogenetically oldest vertebrates and has been conserved for over 560 million years (Stephenson-Jones et al., 2011).

Several studies have shown that lesions of different cellular components of the BG lead to severe neurological disorders such as Parkinson's and Huntington's disease (Alexander et al., 1986; Albin et al., 1989). Furthermore, there is growing evidence that dysfunctions in the BG circuitry can be implicated in several neuropsychiatric disorders like schizophrenia, Tourette's syndrome, attention deficit disorder and obsessive-compulsive disorder (Middleton and Strick, 2000).

The canonical anatomy of the basal ganglia system (figure 2.3) is composed by the striatum (caudate, putamen and nucleus accumbens), the external and internal segments of the globus pallidus, the subthalamic nucleus, and the substantia nigra *pars compacta* and *pars reticulata* (Gerfen and Bolam, 2010).

The main input structure of the BG is the striatum. The majority of these inputs come from layer 5 glutamatergic neurons from a broad cortical area, but thalamic nuclei and the substantia nigra *pars compacta* also provide strong excitatory and dopaminergic inputs to the striatum, respectively (Gerfen and Bolam, 2010). The striatum of primates is structurally subdivided in three nuclei: caudate nucleus, putamen and nucleus accumbens. However, rodents lack an internal capsule that is the structural separation between the caudate nucleus and the putamen, being these nuclei fused in one single structure denominated caudate-putamen (CPu). Striatal outputs are entirely inhibitory and project to the globus pallidus and substantia nigra.

Another input structure of the BG is the subthalamic nucleus (STN). The STN receives glutamatergic inputs from cortical areas exclusively located in the frontal lobe and essentially responsible for movement and inhibitory input from the external segment of the globus pallidus (GPe) (Squire et al., 2008). Unlike the striatum, the output from STN is excitatory (glutamatergic) and it provides projections to the internal segment of the globus pallidus and substantia nigra *pars reticulata* (SNpr), also projecting back to the GPe.

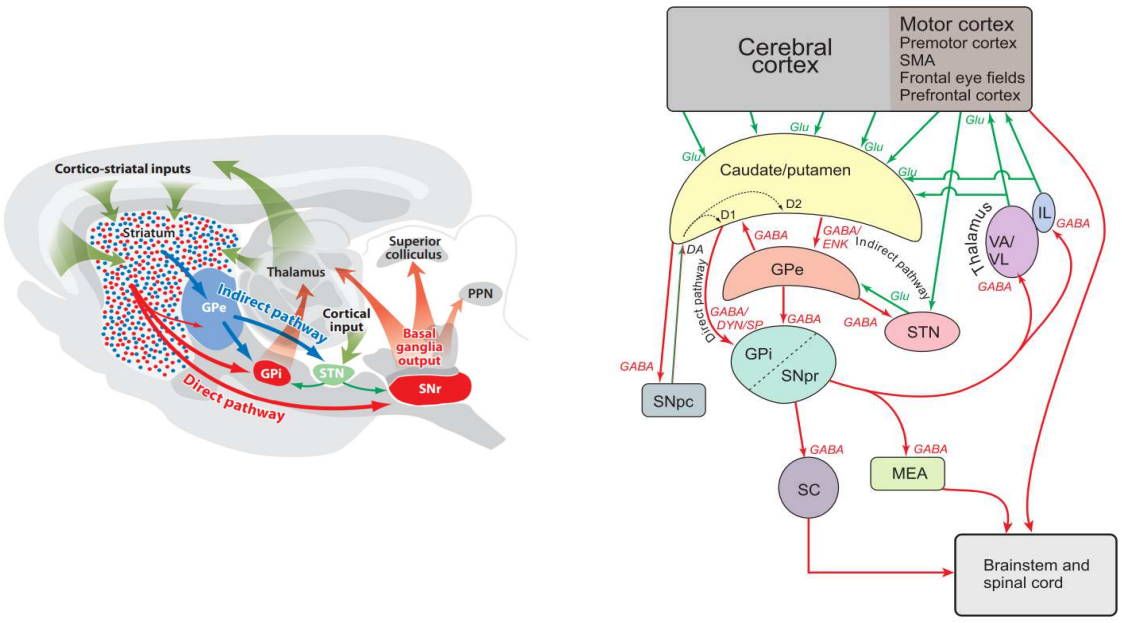

Figure 2.3: Diagrams of the basal ganglia anatomy and neural circuits. Sagittal diagram of the nuclei composing the rodent basal ganglia **(left)** - Adapted from Gerfen and Surmeier (2011). Simplified schematic diagram of basal ganglia circuitry **(right)** - Adapted from Squire et al. (2008)

.

The globus pallidus is divided into two segments: the internal (GPi) and external (GPe) segments. The GPi is an output structure of the BG, being primarily composed of large neurons that project outside of the BG. It receives a large number of distinct inputs mainly from the striatum (inhibitory) and from the STN (excitatory). The neurotransmitter used by the GPi is GABA, meaning that the output of this structure is inhibitory to thalamic nuclei, to the brainstem and also back to the striatum. The GPe is an intrinsic nucleus of the BG as it only receives and sends information from/to other BG nuclei. It receives inputs from the striatum and the STN and it has inhibitory output projections mainly to the STN but also to the GPi, SNpr and striatum.

Similarly to the GP, the substantia nigra (SN) is also divided in two distinct structures: *pars compacta* (SNpc) and *pars reticulata* (SNpr). SNpr receives GABAergic inhibitory inputs from the striatum and glutamatergic excitatory inputs from the STN. Like the GPi, SNpr is also an output structure of the BG, with inhibitory GABAergic projections to the thalamus and to cortical and brainstem areas involved in eye movement control. SNpc is composed by a large population of dopaminergic neurons that receive and send information from/to the striatum, modulating its activity.

A schematic of the BG circuitry and its main connections is illustrated on the right panel of figure 2.3.

2.3.2 Striatal Neurons

The target structure studied in this project is the basal ganglia's largest component and main input: the striatum. The neurons composing the striatum have been studied and characterized (Wilson and Groves, 1980), with four major types of neurons being described based on anatomic, histochemic and

physiological differences (Squire et al., 2008).

The most abundant neuron type in the striatum is the medium spiny neuron (MSN), making up 80 to 95 % of the total number of striatal neurons (Oorschot, 1996). These neurons are the main receiver of external input and are the only type of output neurons of the striatum (Wilson and Groves, 1980). The output of MSN is exclusively GABAergic, with axonal projections to both segments of the GP and SN, as described in the previous section.

The remaining three types of striatal neurons are quite less prevalent than MSNs and, unlike MSN, are anatomically characterized by absence of dendritic spines (aspiny neurons). These aspiny neurons are interneurons that use different neurotransmitters and which axon collaterals mainly terminate in MSN. Large aspiny neurons use acetylcholine as a neurotransmitter; medium aspiny neurons are thought to use somatostatin and to release other chemicals such as substance P or enkephalin; and small aspiny neurons are GABAergic intraneurons (Squire et al., 2008). Like MSNs, striatal interneurons also receive glutamatergic input from both cortex and thalamus, although less abundantly as these inputs mainly terminate on the dendritic spines of MSNs (Kemp and Powell, 1971). On the other hand, the output of these interneurons is essentially directed to MSNs and other interneurons. Consequently, striatal interneurons play an important role in regulating the activity of MSNs, being crucial in modulating both striatal inputs from the cerebral cortex and striatal output (Squire et al., 2008).

In addition to cortical, thalamic and intraneuron inputs, MSNs are also the target of dopaminergic neurons from subcortical regions such as the ventral tegmental area (VTA) and the SNpc (Smith et al., 1994).

The effect of dopamine inputs depends on the type of dopamine receptors expressed by the striatal neurons. There are five different G protein-coupled dopamine receptors (D1-D5), grouped in two families according to their responses to agonists. The D1 family is composed by D1 and D5 receptors, which are associated with an excitatory response to dopamine due to its coupling to a Gs-protein. On the other hand, receptors from the D2 family, which includes the remaining D2, D3 and D4 receptors, by being structurally coupled to Gi-proteins, produce inhibitory responses to dopamine and other agonists (Stoof and Kebabian, 1981).

Taking into account the different expression of dopaminergic receptors and different axonal projection targets, the MSNs are commonly divided into two distinct subpopulations, which give rise to two parallel BG circuits: the direct and indirect pathways. The direct pathway is composed by MSNs that directly project to the output nuclei of the BG (GPi and SNpr) and primarily express D1 receptors. A second population of MSNs constitutes the indirect pathway and it mainly expresses dopamine receptors from the D2 family. Instead of sending direct projections to the BG output structures, these neurons project neurons in the GPe, which then project to the STN, whose neurons finally project to the SNpr and GPi.

The direct and indirect pathway model of the BG has been extensively studied, specifically in the understanding of the role of these pathways on motor control. A classical view proposes that these two pathways exert opposing influences on motor functions: excitation of the direct pathway contributes to the facilitation of movement and the activation of the indirect pathway potentiates movement inhibition (Kravitz et al., 2010).

2.3.3 Peltier Effect

The Peltier effect is a thermoelectric effect observed for the first time in 1834 by Jean Charles Athanase Peltier, a french watchmaker. A thermoelectric effect is characterized by the conversion of electric current into temperature gradients and vice versa through the junctions of two dissimilar electrically conductive materials, commonly mentioned as a thermocouple (Goldsmid, 2010), (Bell, 2014).

Peltier found that if an electric current passes through a thermocouple, either a heating or cooling effect occurs at this junction and when the direction of the electric current applied is reversed, the opposite thermal effect is observed.

The application of this effect was practically none for over one century until the development of semiconductor materials, which have properties that enable the production of considerably larger thermal gradients than metals (Riffat and Ma, 2003). Semiconductors are materials with special electrical properties as they have a charge flow that cannot be fully captured by the definition of electrical conductors or insulators.

These conducting properties can be extrinsically manipulated by introducing impurities into the semiconductor crystal structure, disrupting the equilibrium between the number of free electrons and holes. A semiconductor is said to be n-type if the number of free electrons in the lattice is bigger than the number of holes and a p-type if this inequality is the other way around (Sze and Ng, 2006).

In a thermoelectric device based on the Peltier effect, p- and n- type semiconductors are alternated between two plates, so that heat is pumped from one plate (the cold plate) and into another (the hot plate) as current flows through the device (Aronov and Fee, 2011). Figure 2.4 shows a schematic of the electric and heat flow between two plates connected by a p- and n-type semiconductors pair.

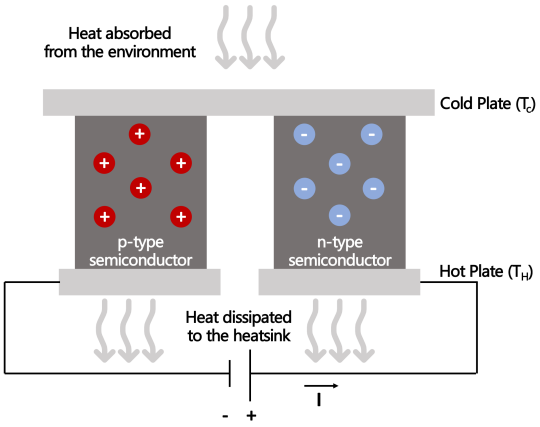

Figure 2.4: Schematic of the Peltier effect. Thermoelectric module operation in the cooling mode (direction of the current (I) from the n-type to the p-type semiconductor), with heat being extracted from the environment in contact with the cold plate and transferred to the hot plate through an n-p pair of semiconductors - Adapted from Riffat and Ma (2003).

In this schematic, the current applied is passing from the n-type to the p-type semiconductor. As a result, the temperature of the conductor plate connecting the semiconductors decreases as heat is being absorbed from the environment (cold plate). The absorbed heat is transferred through the semiconductors to the other plate (hot plate), which increases its temperature (Riffat and Ma, 2003). When the direction of the applied current is reversed, the opposite effect is observed, reversing the hot and cold plates, hence the environment from which heat is being absorbed.

2.4 Theoretical Hypothesis

Motivated by the findings of Gouvêa et al. (2015) providing remarkable evidence that striatal dynamics encode the timing information that rats were using to guide their judgments while performing a psychophysical task, our study intends to causally manipulate in a dose dependent and bidirectional manner the speed of striatal population dynamics and get insights on it impacts the animals judgment of elapsed time.

Hereby we propose that reversibly cooling or heating the temperature of striatal tissue, hence locally slowing down or speeding up neural activity in the striatum, will induce behavioral changes in animals' judgments in the context of an interval categorization. We believe that manipulating striatal temperature will bidirectionally affect estimates of elapsed time, making animals more likely to judge near boundary stimuli as long or short if the temperature is warmer or colder than the physiological body temperature, respectively (figure 2.5).

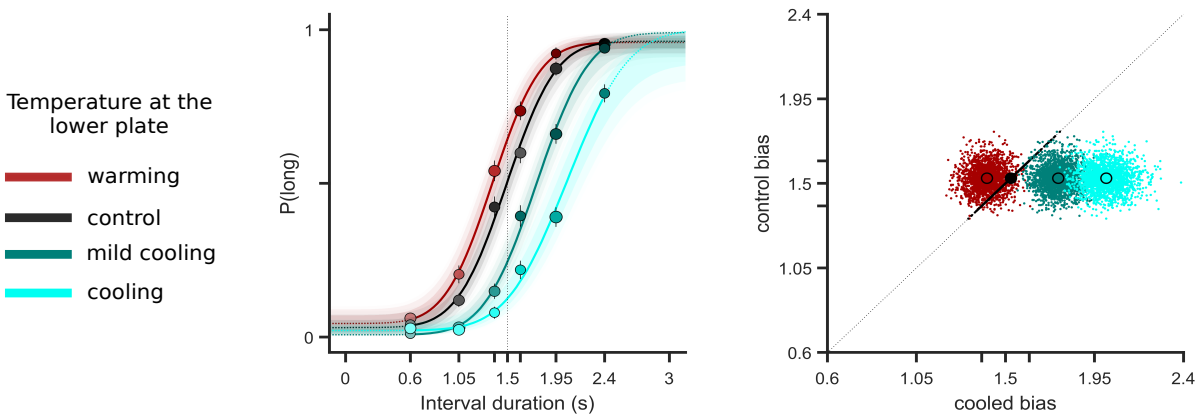

Figure 2.5: Data simulation of the theoretical hypothesis. The simulation was done with 2000 sessions with an average of 500 trials. Red, teal and cyan qualitatively represent three different manipulation doses ordered from the warmest to coldest **(left)**. Psychometric curves from trials separated according to temperature label. Data points represent the mean proportion of long choices $\pm$ standard error of mean (s.e.m) for each stimulus duration and are fitted with a 4-parameter logistic function **(middle)**. Thresholds defining the psychometric curves of each dose for each session plotted against the corresponding control threshold.

Chapter 3

Methods

3.1 Subjects

The study was performed in 4 Specific Pathogen Free (more information at `http://www.felasa.eu`) male Long-Evans hooded rats (*Rattus norvegicus*) - Alan, Chandler, Joey and Roger. At the time of the surgery, their ages ranged from 11 to 13 months and their weights from 487 g to 552 g. All rats were wild type except Roger. The differences in genotypes were not considered relevant in the behaviour analysis made.

Until surgery, animals were kept in pairs in transparent cages with HEPA (High-Efficiency Particulate Air) filters on a 12 hour light-dark cycle (with lights ON at 8am), at 21 ^{o}C and relative humidity of 50%. All experimental procedures were performed during the light phase of their cycle. Animals were identified by the different spot patterns in their furs, for the purposes of behavior, data and MRI analysis.

During the whole experimental period, animals had *ad libitum* access to food and were water deprived, getting access to water daily during 2 hour-long behavioral sessions.

All experimental procedures were carried out according to the European Directive 2010/63/EU and were approved by Portuguese Veterinary General Board (Direcção-Geral de Alimentação e Veterinária (DGAV), project approval 0420/000/000/2011 and 0421/000/000/2018).

3.2 Experimental Setup

Both behavior training and manipulation procedures were carried out in two identical 42.0 x 30.0 x 35.5 cm polypropylene boxes (Ikea, Sweden) (figure 3.1, left). The boxes had a custom laser cut 3 mm thick acrylic floor to prevent rats from gnawing directly on the box's floor and were covered with a lid to minimize the contact with the exterior that could lead to animals' distraction or escaping. The lids were made of acrylic and had stripes of red light-emitting diodes (LED) glued to the part facing inside the box. These lights allowed video recording of behavioral sessions (see below), preventing rats' distraction as they cannot see the wavelength of red light in the visible spectrum.

Each box had three equidistant cylinder-shaped nose ports (Shapeways, USA) placed in one of the

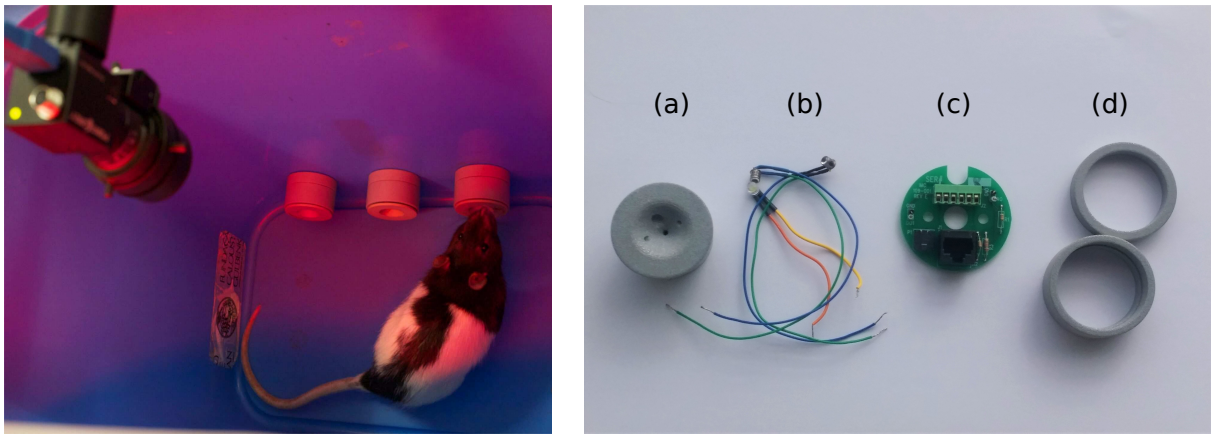

Figure 3.1: Experimental setup and main components of a nose port. Animals perform the task inside a box with three nose ports. Trials are initiated in the center nose port and choices are reported to one of the side ports, where water reward is available upon correct choices. A video camera is hanging on top of the box to collect video data during the behavioural task **(left)**. Mechanical and electronic components of the nose ports **(right)**. **(a)** Nose port mechanical structure. LEDs are placed in the peripheral holes and water rewards are delivered through a spout placed in the central hole of this structure. **(b)** White light LED and infra-red LED emitter and receiver. The infra-red LEDs are facing each other and placed just before the hole of the port in order to detect entries in the port. **(c)** Custom printed circuit board that connects the nose ports to a board controlling the behavioral sessions. **(d)** Structural rings fo the nose port.

wider walls of the box, allowing the rats to place their snouts inside: one in the center and the other two symmetrically displayed on the left and right side of the central poke (figure 3.1, left).

As illustrated in right panel of figure 3.1, the nose ports (or pokes) were composed by different structural and electronic components:

- A white LED on the top centre of the poke (Farnell, Portugal) - figure 3.1 (b);
- An infra-red LED emitter (Farnell, Portugal) and an infrared LED receiver (Farnell, Portugal), facing each other, one of each side of the white LED, to detect snout entries inside the poke - figure 3.1 (b);
- A custom printed circuit board (PCB) (made by the Champalimaud Hardware Platform), that connected the above-mentioned components to a second board, which controlled the experimental task - figure 3.1 (c);
- A solenoid valve on the side pokes (The Lee Company, USA) connected to a metal spout that delivered water rewards through a hole;
- 2 rings that not only gave structure to the poke but also protected its components from being bitten by the ratsfigure 3.1 (d).

Apart from the nose ports, which were the rats' interface to report a choice and collect rewards, there were other components in the setup:

- A speaker (Monacor, Germany) that played different tones along the task.

- Silicone tubing ($\frac{1}{8}$ inches outer diameter, Cole-Parmer, USA) connected on one end to the solenoid valve and on the other end to a 20 mL syringe containing water.

- A video camera (Point Grey Flea 3.0, recording at 60 fps, with 1.2 MPx resolution) hanging on top of the box to collect video data during the behavioural task - figure 3.1, left panel.

These hardware components (except for the camera) were monitored by sensors and controlled by actuators by a microcontroller board (Arduino Mega 2560), through a second custom-made PCB (made by the Champalimaud Hardware Platform), with inputs and outputs for the LEDs, water valves and speaker.

The Arduino was connected to a computer running Windows 10, via a serial communication port (USB cable). On this computer, a sketch written using the Arduino 1.8.5 integrated development environment (IDE) (additional information and free software available at `http://www.arduino.cc/`) implemented the state machine that controlled all behavioral assays. The behavior experiments were mostly automated, needing minimal intervention of the experimenter: a task started with the Arduino sketch upload followed by the opening of a custom software based on Python's pySerial module (freely available at `http://pyserial.sourceforge.net/`), which saved the behavioral data in a text (.txt) file.

3.3 Behavior

The four rats were trained to categorize time intervals as either long or short by making left/right choices, respectively (Gouvêa et al., 2014).

Animals were trained in 2 hour sessions, 5 days per week. Training lasted approximately 2 months (see section 4.2) and consisted of different training stages leading to the final task.

One day before starting training, animals were weighted (to register a baseline body weight) and water access was taken from their cages. At the beginning of every training session, rats' weights were registered in a spreadsheet, allowing us to monitor their health by guaranteeing the weights would never go below 80 % of their baseline.

3.3.1 Training Stages

Before learning the interval categorization task, animals were taught how to interact with the nose pokes, through different training stages.

During the first training stage, animals learned to initiate a trial in the central nose port, which was the only one illuminated. When inserting their snout in the central port, a 7 kHz tone was played and both left and right ports lit up and the animal could collect a reward at any of the edge pokes. Once they learned that a trial is started in the central poke and that reward is available on the side pokes, animals were moved to the next training stage.

During training stage 2, after initiating trials, the same tone as in stage 1 was played but now only one of the side pokes lighted up and was rewarded water and after a 1.75 kHz tone was played.

The last training stage aimed to teach the animals how to fixate in the center poke (break the infra-red beam in a sustained manner) for a progressively larger period of time before starting a movement to one of the side ports.

When initiating a trial, a 7 kHz tone was played and the animals were required to stay still (fixating) at the nose poke until a second identical tone was played, allowing them to leave to one of the side ports, where a reward was available. On the first day of this training stage, each trial with a successful fixation resulted in an increment of 10 ms on the fixation interval of the subsequent trial. If the animal failed to fixate in one trial, the interval would decrement 5 ms.

From session to session we adjusted the parameters to each animal individually. The minimum fixation time and the increment time were increased until the animals were able to reliably reach a fixation time of 2500 ms, early within a training session.

3.3.2 Interval Categorization Task

Animals were trained 5 times a week in 2-hour sessions in a Two-Alternative Forced-Choice (2AFC) task to categorize the interval duration between two tones as either long or short by reporting left or right choices, respectively (figure 3.2, left).

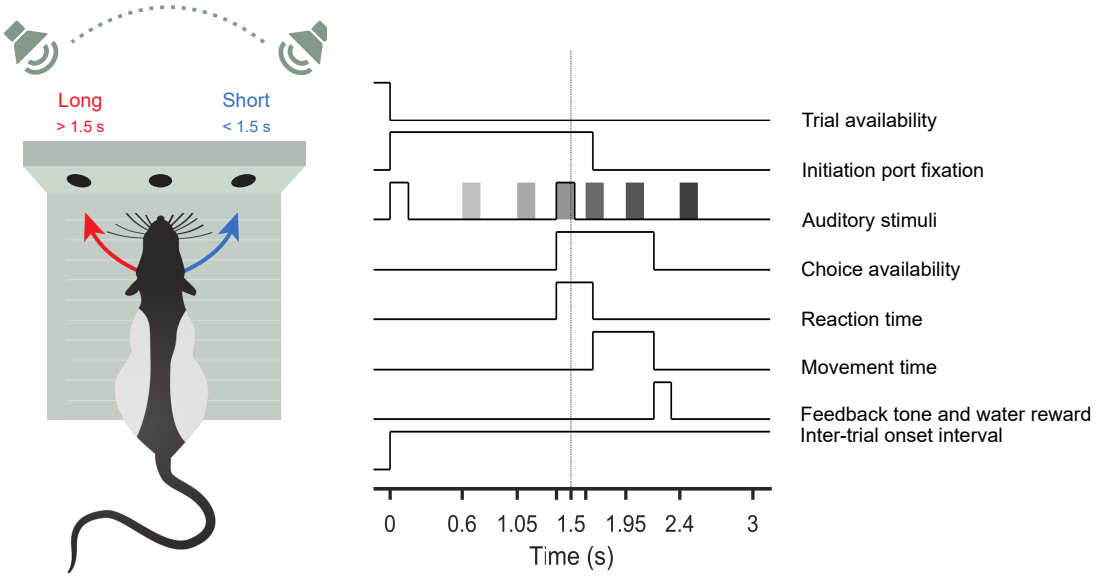

Figure 3.2: Interval categorization task. Rats judged interval durations as either longer or shorter than a 1.5 s categorical boundary. Long judgments are correctly categorized if reported on the left port and short judgments should be reported to the right port of the box. Rats triggered interval stimuli (i.e. two brief auditory tones separated by a silent interval of random duration sampled from a 6 stimuli set) by inserting their snout into a central port. During the interval between the two auditory tones, animals were required to fixate (i.e, to keep interrupting the infra-red light beam) inside the nose port. Following interval offset, animals reported either a short or a long judgment at two lateral choice ports. Correct trials yielded a water reward, while incorrect or premature responses produced a white noise sound and a time out. Left panel shows a schematic of the task and the right panel shows an event diagram of the task.

A trial was initiated when rats nosepoked the illuminated central nose port, triggering a stimulus interval. Triggering a stimulus immediately turned off the initiation port light and played a pair of audible tones

separated in time by an interval randomly selected from the set $I = \{0.6, 1.05, 1.38, 1.62, 1.95, 2.4\}$s, with uneven sampling probabilities: the more difficult the stimulus, the more likely it was for it to be presented in a trial. Tones consisted of 150 ms long trains of square pulses at 7 kHz. The six time intervals in the above-mentioned set I are symmetrically distributed around the 1.5 s categorical boundary and define three difficulty levels: the further a stimulus is relative to the 1.5 s boundary, the easier it is to correctly categorize it.

A new trial could be initiated once the initiation port became illuminated again. This inter-trial interval varied according to the choice in the previous trial. For correct trials, a new trial was available 9 s after the initiation of the previous trial (inter-stimulus onset interval). For incorrect trials/broken fixations, the inter-trial interval was 19 s and 24 s, respectively.

Rats were required to withhold nose poking at the central port during the period of time between the two tones, corresponding to the stimulus duration on that trial. Fixations broken before interval offset were penalized with an error tone (150 ms white noise sound) and a 15 s time out. For intervals longer/shorter than the categorical boundary, a 25 μL water reward was delivered and a 1.75 kHz tone was played upon choice of the left/right nose port, respectively. Incorrect choices resulted in a white noise sound and were punished with a 10 s time out. If the animals fail to categorize the same stimulus three consecutive times along the session, they enter in a correction loop, where the same incorrectly categorized stimulus is the only being drawn in the next consecutive trials. In this state, each correct trial discounts the number of further trials with the same stimulus, until the animal leaves the correction loop. On the other hand, incorrect trials are penalized with one more trial in which the same stimulus is being drawn. Therefore, the animals leave a correction loop state after giving the same number of correct answers as incorrect to a specific stimuli.

The main behavioral readouts from this task are the reported choice, reaction times and movement times. The reported choice corresponds to the side port which infra-red light beam was interrupted after leaving the central port (left or right). In the context of this task, a reaction time is defined as the time the animal takes to leave the central nose port (and the infra-red light beam is no longer interrupted) after the second tone is played. Movement times correspond to time interval between the moment an animal leaves the central nose port and when a choice is reported in one of the side nose ports (with the interruption of the respective infra-red light beam).

An event diagram summarizing the task can be seen on the right panel of figure 3.2.

3.4 Thermoelectric Cooling (TEC) Device

3.4.1 Design and Architecture

We built a custom-made implant based on the Peltier effect to systematically manipulate the temperature of brain tissue of rats (figure 3.3).

The design and assembly of the implant took into account the performance of five different modules: heat dissipation, thermoelectric (TEC) device, temperature monitoring, heat transfer and heat insulation.

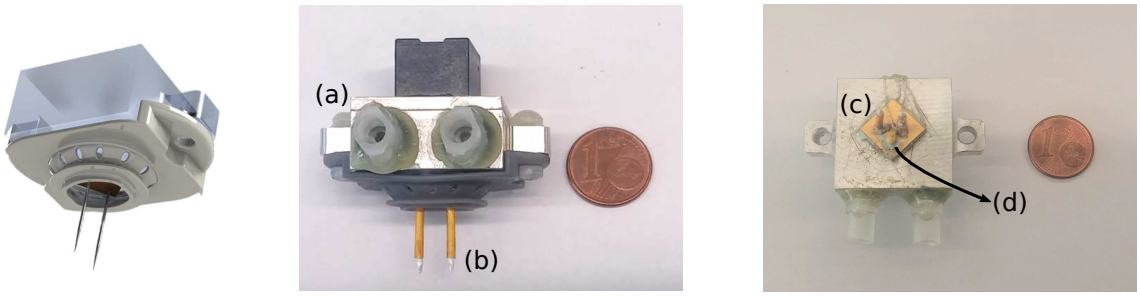

Figure 3.3: Implant architecture. The panel on the left shows a 3D model of the implant (courtesy of Paulo Carriço, Champalimaud Hardware Platform) and both middle and right panels show pictures of the final version of the implant taken from a front and a bottom perspectives, respectively. The main components of the implant are: **(a)** the active cooling heatsink, with luer lock fittings glued to its inlets and outlets; **(b)** two sharpen silver probes insulated down to the tips with a layer of polytetrafluoroethylene and polyimide tubes; **(c)** a thermoelectric module with one of the plates glued with thermal glue to the heatsink. **(d)** a thermistor glued with thermal glue to the lower plate of the thermoelectric module, allowing temperature control and readout at this plate.

During an optimization phase, performance of implants was compared in terms of dynamic range of temperature, long-term stability and over-heating of the implant was conducted (see subsection 3.4.3). Moreover, the dimensions and weight of the implant were also a limiting factor since the animals would still have to perform the behavioral task after being chronically implanted (we kept it under 10 % of animals' body weight).

The overheating of the peltier, hence the temperature stability over time, was overcame using an aluminium active cooling heatsink (21 g, 25.4 mm x 25.4 mm x 12.4 mm, Custom Thermoelectrics, USA). Room temperature water was inserted through the inlet of the heatsink and travelled through the several chambers (total volume of 1.61 mL) of the water block, absorbing the heat from the hot plate of the peltier and exiting the heatsink through an outlet. The water was being pumped at a constant flow (approximately 15 mL/min) by a peristaltic pump (Williamson, United Kingdom).

A thermoelectric module (Custom Thermoelectrics, USA) was glued with thermal glue (Farnell, Portugal) on one of the widest sides of the heatsink. The peltier had 48 semiconductor couples of Bismuth Telluride (Bi_2Te_3) connecting two 10 x 10 mm alumina ceramic with copper/nickel and gold plating plates.

Temperatures were measured by a thermistor (Farnell, Portugal) glued with thermal glue to the plate of the peltier that was not glued to the heat sink and the Steinhart-Hart equation (Bell et al., 2003) was used as the model to describe the resistance of the thermistor at different temperatures.

To conduct heat to the target tissue, two silver probes (length = 15 mm; diameter = 1 mm; k = 428 $Wm^{-1}K^{-1}$ (Tilley, 2004)) were soldered 5 mm apart with silver and lead solder to the same plate where the thermistor was glued. The distance between probes was defined according to the target region in the animals brains, which is roughly 2.5 mm to each side (ML) from Bregma. To facilitate the implant placement during surgery, both tips were sharpened in a rolling sharpening stone. To minimize heat exchanges along the length of the probe and hence improving the efficiency of the device in producing temperature changes deep in the brain, poor thermal conductors were selected for insulating the probes. Both silver probes were insulated with a layer of polytetrafluoroethylene (teflon)(k = 0.27

$Wm^{-1}K^{-1}$ (Han and Fina, 2010)). Furthermore since the air has very low thermal conductivity (k = 0.025 $Wm^{-1}K^{-1}$ (Aronov and Fee, 2011)), we chose to insulate probes with polyimide tubes (diameter = 1.1 mm; k = 0.12 $Wm^{-}1K^{-1}$ (Aronov and Fee, 2011)) that were glued at the beginning and end of the polytetrafluoroethylene layer, and were wide enough to leave some air between the probe covered with teflon and the polyimide wall.

A 6 pin female RJ45 connector (Farnell, Portugal) was glued with epoxy (Araldite, Farnell, Portugal) to the heatsink. The thermistor and peltier were soldered to individual pins, allowing the temperature control and readout of the thermoelectric device.

3.4.2 Temperature Control and Readout

The implant was connected to a custom-made PCB (made by the Champalimaud Hardware Platform), which was connected to an Arduino Mega 2560 microcontroller. Both the PCB and the Arduino were connected to a computer running Windows 10.

A LabView-based graphical user interface (GUI) developed by the Champalimaud Hardware Platform (TEC visualizer) allowed us to read temperature at the plate of the peltier where the thermistor was glued. The temperature was sampled at 100 Hz, saved to a text file and plotted by the software, providing a prompt visualization of temperature fluctuations.

The lower plate of the peltier was set to different target temperatures in a closed-loop fashion using a proportional–integral–derivative (PID) controller implemented in the custom-made PCB. The temperature measurement at the thermistor and the currently set target temperature were continuously compared in order to compute an absolute error term (proportional channel), a cumulative error (integrative channel) and an instantaneous change in error (derivative channel). The three error terms were then linearly combined (weights set by the resistive and capacitive components of the hardware modules that implement them) and used to modulate the control current driving the TEC. This negative feedback mechanism was optimized so that the target temperature could be reached with minimal delay, no steady-state errors and with negligible overshoot.

The different manipulation temperatures, the duration of a block with the same temperature and the steepness of the transitions between temperatures were defined in the Arduino program.

Since the manipulation was being done in living biological tissue, temperature change in the lower plate during the experiments was limited to a range between 10 ^{o}C and 45 ^{o}C. To prevent over or undershoots off these limits that could compromise the animals' well-being, a failsafe mechanism was implemented in the board's microcontroller. This safe system would disable the device if any temperature below 0 ^{o}C or above 55 ^{o}C was registered.

3.4.3 Testing

All different implant architectures were tested at room temperature by setting them to different target temperatures ranging from 0 ^{o}C to 42 ^{o}C, while the temperatures at the heat sink, the lower plate and both silver tips were registered during blocks of 5 minutes.

The final version of the implant (see figure 3.3, middle) underwent a second round of testing, in which agarose at 37 ^{o}C was used to mimic the thermal properties of brain tissue (Kim et al., 2007). A heating pad connected to a direct current (DC) temperature controller (FHC, USA) through a closed-loop feedback system was placed under a small piece of agarose (2% (V/V)), keeping its temperature constant at 37 ^{o}C (approximately the body temperature of a rat). The peltier tips were placed inside the heated agarose and measurements of the temperature at the tips and at the lower plate were registered for 5 minutes.

All the implants that ended up being implanted were assembled and tested in the same manner in order to guarantee similar performance. Furthermore, transfer functions between both the set and measured temperatures at the lower plate and the measured temperature at the tips were calculated.

3.5 Surgical Procedure

The rats underwent surgery after 3 months of training the task described in section 3.3.

During the implantation of the device rats were anesthetized with 2.0 - 4.5 % isoflurane. The animals' body temperature was continuously monitored and maintained by a rectal probe connected to a closed-loop feedback heating system (FHC, USA).

After being anaesthetised and before making the first incision, we administered subcutaneously Vetacort (1 mL), Rimadyl (0.5 g/Kg) and a saline solution of atropine (0.1 mL/100 g) .

We stereotaxically targeted the striatum bilaterally (+ 0.84 mm AP, $\pm$ 2.5 mm ML, - 4 mm DV from Bregma - figure 3.4) and two craniotomies and durotomies matching the diameter of the silver probes were made. 6 support screws were placed: 3 in the occipital plate and 3 anterior to the location of the craniotomies. The cranial bone was covered with SuperBond (Locite) to improve adherence to the dental acrylic used to secure the implant.

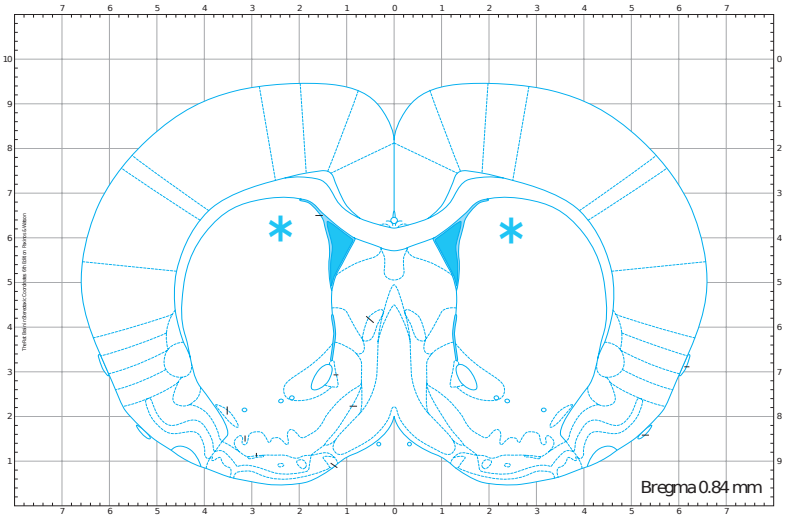

Figure 3.4: Coronal view of the implant targeting the dorsal-central striatum. Target locations of each one of the probes are represented in the atlas figure with the blue stars (+ 0.84 mm AP, $\pm$ 2.5 mm ML, - 4 mm DV from Bregma) - Adapted from Paxinos and Watson (2006).

The striatal cooling device was then slowly lowered perpendicularly to the brain surface to a depth of 4 mm from cortical surface. It was fitted into place and secured with several layers of dental acrylic (the first one mixed with gentamicin - antibiotic prophylaxis).

The procedure ended with suturing with Vicryl the skin anterior and posterior to the implant.

After surgery animals were individually housed in double decker cages without the second level to minimize implant damage. During the 3 days following surgery, animals were injected once a day with Rimadyl (0.5 g/Kg). Animals were allowed to recover for a week after the surgery with food and water *ad libitum*.

3.6 Manipulation Sessions

After one week recovery from surgery, all the animals were again water deprived, a new baseline weight was registered and the rats restarted daily training sessions (7 days per week).

After reaching stable performance, behavioral sessions were divided in 3-minute fixed-time blocks: control blocks, in which the peltier's lower plate was set to body temperature ($\sim$36 ^{o}C), that were interleaved with different manipulation doses (15, 25 and 45 ^{o}C), randomly selected without replacement. Each session always started and ended with a control block and the animals were not queued when blocks switched.

Manipulation sessions were interleaved with washout sessions, in which the controller of the implant was disabled, and correction loop training was reinstated (see training procedures above, section 3.3).

All manipulation sessions were video recorded with a Flea 3 camera (Point Grey) using Bonsai (software available at `http://www.open-ephys.org/bonsai`).

3.7 Data Analysis

All data were analysed in MATLAB 2018a (additional information at `https://www.mathworks.com`).

To fit the behavioral data showing the probability of making a long choice as the function of the duration of presented stimulus intervals, we used logistic psychometric functions as described in the work of Schütt et al. (2016), using their *psignifit* tool box (Equation 3.1).

$$\psi(x; m, w, \lambda, \gamma) = \gamma + (1 - \gamma - \lambda)S(x; m, w) \tag{3.1}$$

where $S(x; m, w)$ is the sigmoid

$$S(x; m, w) = \frac{1}{1 + \exp\left(-2 \times \frac{\log(\frac{1}{0.05})-1}{w}\right)(x - m)} \tag{3.2}$$

In this logistic regression fit, w is mathematically defined as $S^{-1}(0.95) - S^{-1}(0.05)$, controlling the slope of the function between these performance values. m defined as $S^{-1}(0.5)$ and defines the inflection point or bias of the sigmoid function. Finally, two none psychophysical parameters (γ and λ)

are responsible for the scaling of the sigmoid function defined by m and w. γ gives the lower bound of $\psi(x; m, w, \lambda, \gamma)$, which can be interpreted as the base rate of performance in absence of a signal and λ represents the lapse rate. Both sigmoid and psychometric curves defined from equations 3.1 and 3.2 are depicted in figure 3.5.

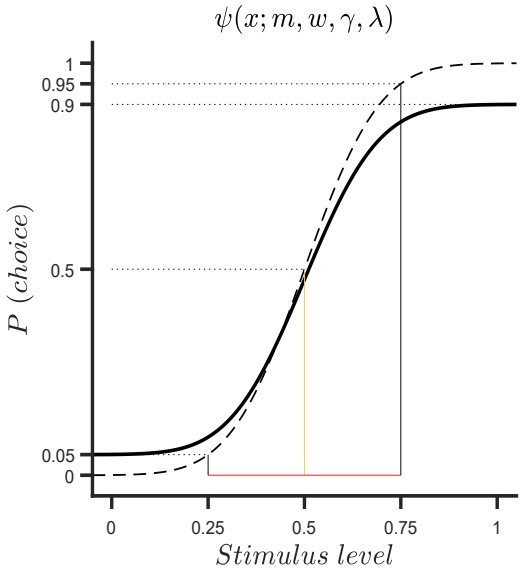

Figure 3.5: Psychometric functions provide readily interpretable quantities that summarize behavior in 2AFC tasks. The curves are characterized by the following parameters: threshold (m) is the stimulus level at which the unscaled logistic function (black dashed line) reaches 0.5 (value at the x-axis marked by the yellow line); width (w) is the difference between the stimulus levels for which the unscaled function reaches 0.95 and 0.05, respectively (length of the red line); λ is defined as the difference between the upper asymptote and 1 and γ is the difference between the lower asymptote and 0. The solid black line represents psychometric function implemented with a logistic fit - Adapted from Schütt et al. (2016).

3.8 Perfusion

Two rats were sacrificed with transcardiac perfusion with phosphate-buffered saline (PBS), followed by 4 % (wt/vol) paraformaldehyde (PFA). Following perfusion and for the remaining two animals, who died unexpectedly, brains were left in 4 % PFA for 24 h and then moved to a 30 % sucrose solution (wt/vol) in PBS for 2 to 3 days.

3.9 Magnetic Resonance Imaging (MRI)

A 1 T (ICON, Bruker) MR scanner was used to collect MRI data. All images were kindly acquired by Francisca Fernandes from the Champalimaud Neuroplasticity and Neural Activity laboratory.

After brain extraction and perfusion or PFA immersion, a T_2-weighted structural image of the brains was collected using a Rapid Imaging with Refocused Echoes (RARE) pulse sequence. The sequence used had a repetition time (TR) of 2800 ms, echo time (TE) of 90 ms and a RARE factor of 12.

The field of view was set to 28 x 15 x 20 mm^3, the spatial resolution of the images was 150 x 150 x 150 μm^3 and a matrix of 187 x 100 x 133 voxels was acquired after 8 averages during a $\sim$7 hours scanning.

Chapter 4

Results

4.1 TEC Device Testing

Before Implantation

After settling for a final implant architecture, all seven built implants underwent a testing procedure before performing surgeries.

On a first approach, these tests allowed us to confirm that 6 out of 7 implants were able to convert current into a temperature difference between both plates of the Peltier module and that this difference was conserved, albeit to a lesser extent, between the upper plate and the tips of the probes. Additionally, when set to different temperatures from a sampling set with temperatures between 0 ^{o}C and 42 ^{o}C, all the 6 working implants reached the same temperatures at the lower plate and at the tips, meaning that not only were the implants working but also that their performances were equivalent.

Once we selected the usable peltiers and guaranteed that their working range was equivalent, we wanted to have a better sense about the device's performance inside a brain. For that purpose, we tested the peltiers in agarose (2 % (V/V)) kept constantly at 36-37 ^{o}C with a DC closed-loop temperature controller, mimicking thermal properties of neural tissue (Kim et al., 2007). In figure 4.1 it is shown that there is an offset between the temperature at which the device was set and the temperature registered at the tips. This offset was expected *a priori* since the silver tips are not perfect conductors and the insulation is not perfect either, naturally leading to a reduction in the efficiency of the device in producing temperature changes deep in the brain. Furthermore, it can also be noticed in figure 4.1 that the lowest temperature at which the cold plate of the peltier can stabilize is at 5 ^{o}C, even when set at 0 ^{o}C.

Although it was not surprising to see different temperatures at the tips and at the lower plate of the peltier device and despite no thermoregulatory homoeostatic mechanisms are taken into account in this testing, characterizing this function for a set of temperatures in a biological range was an important step towards choosing which manipulation temperatures to use with more principled and objective criteria.

All in all, for the purposes of this experiment, the implants were stable during the 3-minute period of a block and for all manipulation temperatures.

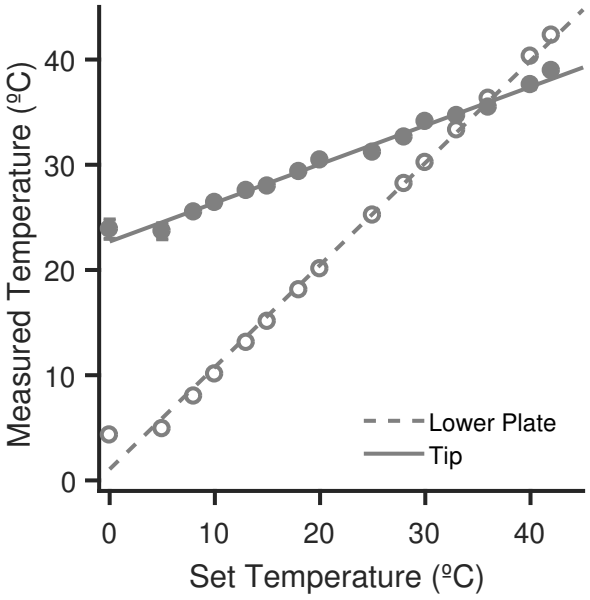

Figure 4.1: Transfer function between set temperatures and measured temperatures at the lower plate and probe's tips. The relation between set and measured temperatures at the tips is represented by the grey circles (mean $\pm$ standard deviation) and between set and lower plate temperatures by the grey circumferences. Data points are averaged during a 5 minute testing period in warmed agarose (2 % (V/V)), and were fitted with linear regressions (dashed line: $y = 0.9705x + 1.0675$, $R^2 = 0.9938$; full line: $y = 0.3677x + 22.7013$, $R^2 = 0.9876$) The manipulation doses used in behavioral sessions were selected according to these tests - 15, 25 and 42 ^{o}C at the lower plate, which approximately correspond to 28, 31 and 39 ^{o}C at the tips, respectively.

Post-mortem

As animals were sacrificed, the implants were carefully removed and re-tested for the manipulation temperatures in warmed agarose. This was done in order to verify that the implants were performing comparably across manipulation sessions.

After visual inspection, all implants were apparently intact and indistinguishable from their pre-surgical state, except for Roger's, in which the thermistor was no longer glued to the lower plate of the Peltier. Since temperature control is done in closed-loop with the thermistor's reading, having air, a poor thermal conductor, in between this now free-to-oscillate sensor and the TEC device's lower plate meant we were no longer operating in the intended temperature range. Consistently, all temperature measurements collected in sessions from this animal were systematically noisier than its counterparts, suggesting it was indeed oscillating. This gave us confidence that this implant was compromised since the first manipulation session, which lead us to remove Roger from the analysis in section 4.3.

The tests of the three remaining peltier implants show that they were still able to achieve temperatures in the range measured before surgeries, suggesting that the peltiers were working across manipulation sessions similarly as when implanted.

4.2 Animal Training

By the beginning of the first stage of training, all animals were naive except for Roger, who had started training four months earlier but had at this point stopped for a period of four weeks.

The first training stage was a process of familiarization with the setup environment and the only criteria to fulfil at this stage was to drink water within a session. Most animals were able to do this after only one session (Figure 4.4, left).

The second stage of training was designed for animals to learn that after initiating a trial in the central poke, they had to fixate - keep breaking the IR beam - until a second auditory go-cue was played. Moreover, at this stage, only one of the reward pokes was illuminated, meaning that the reward was no longer available in both ports but only at the illuminated one. The minimum fixation time and the time increment after a trial with successful fixation were adjusted from animal to animal and from session to session, according to their progress. To adjust these fixation parameters, we analysed animals' behaviour after each training session, using a custom MATLAB script. This script allowed us to monitor the total number of trials initiated in a session, the number of left and right choices, the number of times animals left the central poke prematurely (broken fixations) and the progression of the fixation time across the session (see figure 4.2 for an example session).

After an average of 6 days of training, animals were able to fixate in the central poke for 2500 early in a session (approximately within the first 30 minutes) and to collect reward at the lighted port (Figure 4.4, left). As such, they were deemed ready to start learning the interval categorization task.

The interval categorization task was also divided into different training steps. Firstly, of the stimulus set introduced in section 3.3.2, only the two stimuli of intermediate difficulty (1.05 s and 1.95 s) were presented to the animals. This was done in order to ease the animal into the task while preventing disengagement. Though not strictly necessary, the decision to use these stimuli and not the easiest pair is justified by the concern of having asymmetrical fixation times translate into asymmetric stimulus presentations due to broken fixations. From the left panel on figure 4.4 it can be seen that rats took on average 2 sessions to associate the left reward port to a long interval and the right reward port to short intervals. Subsequently, the easiest (0.6 s and 2.4 s) and hardest (1.38 s and 1.62 s) stimulus pairs were sequentially introduced to the set of possible stimuli in a performance-dependent manner.

Finally, upon reaching close to asymptotic performance, the uniform stimulus sampling distribution (in which all stimuli are equiprobable) used up to this point was replaced by one where sampling probability is proportional to stimulus difficulty. This mechanism, while not adding to any one given trial's demands, has an overall effect on the session's difficulty as it increases the probability of drawing a stimulus closer to the boundary. Therefore, rats were exposed more often to difficult stimuli during a training session.

As an illustrative example of progression across training sessions, figure 4.3 shows the psychometric curves fitting the data of three different sessions of one animal across different training periods after starting the timing task.

Surgeries were done 11 weeks after the beginning of training and animals were considered apt for surgery based on a criteria that took into account the stability of their performances across sessions

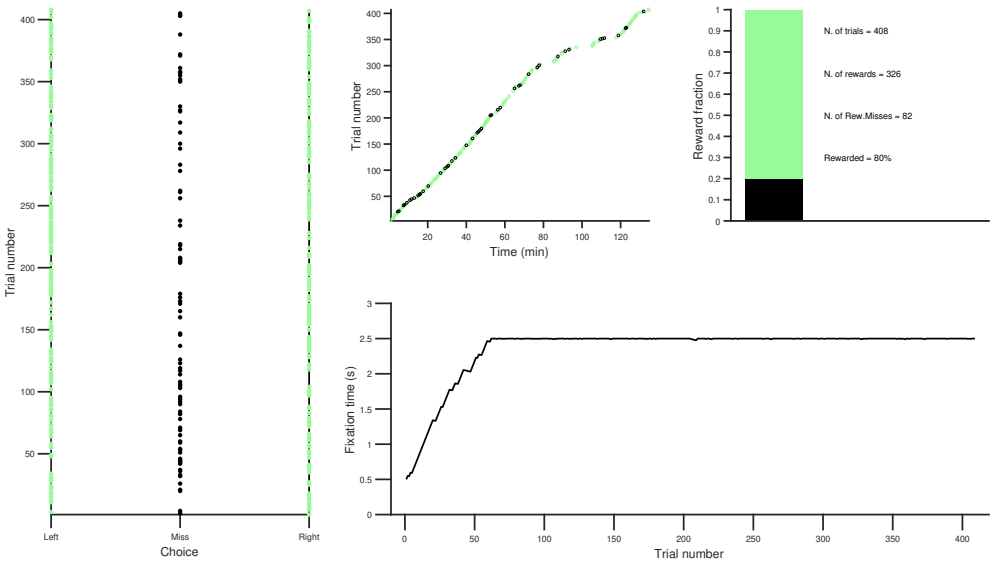

Figure 4.2: Example session from training stage 2. The **left panel** shows the trial history during the session, with trial number for left and right choices in green and trials in which the central poke was left prematurely/broken fixations in black. The **top middle** panel represents the trial history of correct choices (green circumferences) or broken fixations (black circumferences) as a function of time within a 2-hour behavioral session. The **top right** panel shows a quantitative summary of the session with the total number of trials, the number of rewards (correct choices), the number of missed rewards (broken fixations) and the percentage of rewarded trials during the session (number of rewards / total number of trials). The histogram shows in black the fraction of broken fixations and the fraction of rewarded trials during the session. The **bottom right** panel shows the increment/decrement of fixation times during the session: the animal was required to fixate a minimum of 0.5 s. For each correct trial, the fixation time was increased in 50 ms and for each trial where the animals broke the fixation, the fixation time was decreased by 5 ms on the following trial. The maximum fixation time required at this training stage was 2.5 s. This example session corresponds to the last session of Chandler in training stage 2.

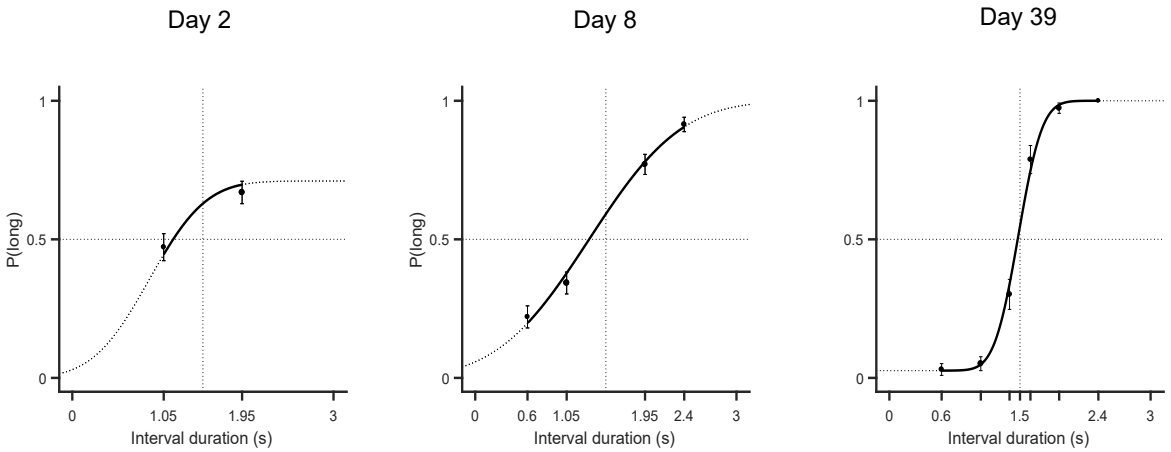

Figure 4.3: Performance evolution in the interval categorization task. The plots represent the mean proportions of long choices for each stimulus ± standard error of mean with the psychometric fits described on the methods. From left to right, each panel shows the performance of an example animal during a session after a different number of sessions since the beginning of training on the interval categorization task.

(over a 70 % performance threshold). This evolution over sessions can be seen on the left panel of figure 4.4.

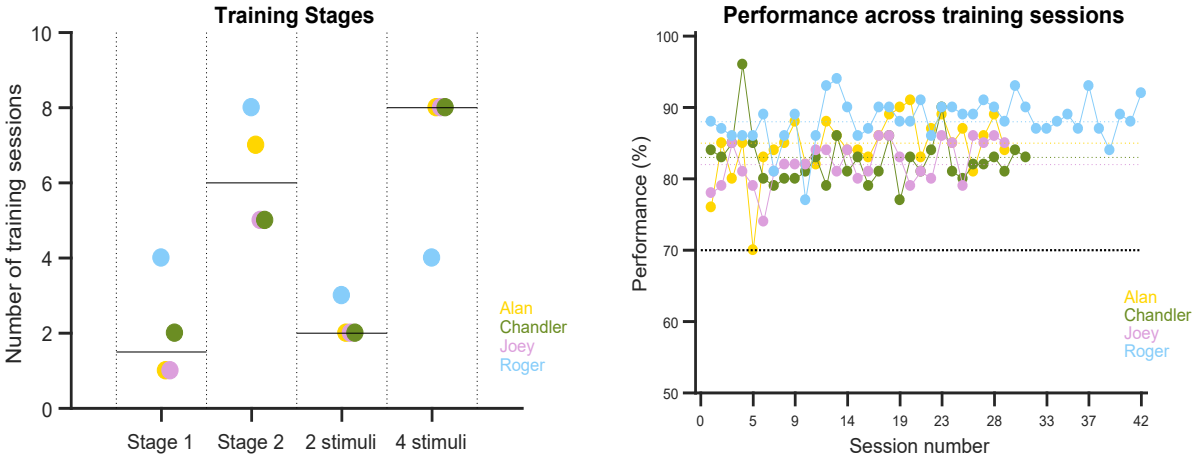

Figure 4.4: Animals progressed similarly across the various stages in our tranining protocol. Number of sessions at each training stage for each one of the four animals. The horizontal black lines represent the median number of sessions **(left)**. Daily performance (number of correct trials/total number of trials) for each animal from the first session doing the complete task until last session before surgery **(right)**. Dashed lines show the individual average performance overall represented sessions. Dashed black line shows the arbitrarily set performance criterion for surgical consideration - 70 % .

The troughs in this performance plot tend to occur on a Monday, the first day of training of the week after a two day break. The influence of stopping training during the weekend was also noticed in the other training stages. This drop in performance could be due to both a break in the daily training routine or to a smaller commitment to the task, since rats were given free access to water for 10 minutes on every pause day. For these reasons, we opted not to advance animals to later training stages on the first session after a pause in training.

By the time of the surgeries to implant the peltier device, all animals showed a consistent discrimination performance in the timing task. The left panel of figure 4.5 shows this stable behaviour over the last three sessions before surgery for all animals.

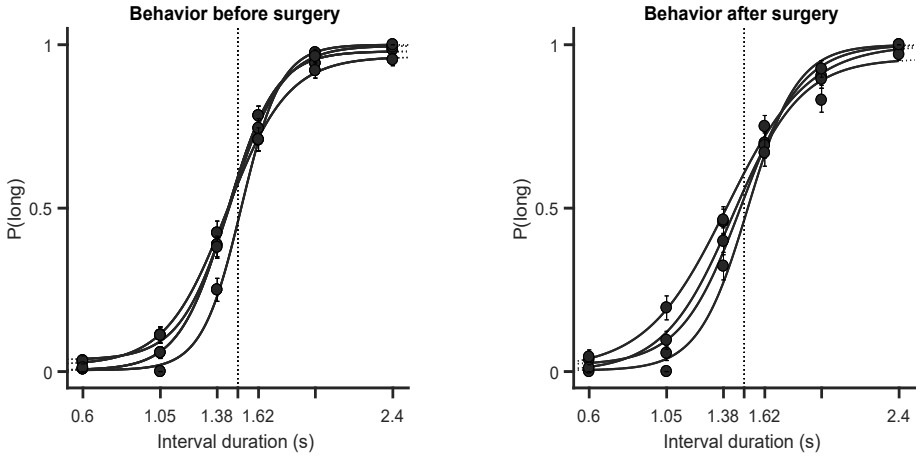

Figure 4.5: Animals showed a consistent behavior performing the interval categorization task before and after the surgeries. Pooled data for the last three sessions before surgeries **(left)** and for the last three sessions before the beginning of the manipulation sessions **(right)** for each animal showing the proportion of long choices (mean $\pm$ s.e.m.) and psychometric fits as described in section 3.1.

Guaranteeing a similar performance and a comparable number of trials per session for all subjects after surgery recovery was also an important step before starting any temperature manipulation procedure. Despite a non-negligible decrease in the number of trials per session (from an average of 407 to 307) there were no marked qualitative differences in the pre- and post-surgery discrimination behavior of the implanted animals (figure 4.5).

All this training and its monitoring led to a highly consistent behaviour and performance in the timing categorization task and thus allowed us to rule out any learning-related but temperature independent non-stationarities when interpreting the effects of our manipulation.

4.3 Behavior in Manipulation Sessions

Animals started temperature manipulation sessions three weeks after the surgery. The manipulation sessions, in which the cooling device was periodically set to different temperatures randomly sampled from a fixed set, were interleaved with "wash-out" sessions, in which the device was disconnected and no temperature manipulations were made. The temperature set from which temperatures were drawn corresponded to temperatures at which the lower plate of the peltier device was set: 42, 36, 25 and 15 ^{o}C. However, from the transfer function shown in figure 4.1, we estimate that the temperatures at the tips of the implant, and hence at the striatal tissue, were around 39, 36, 31 and 28 ^{o}C, respectively. Importantly, in order to prevent having to deal with serial dependencies between the different manipulation temperatures and make sure all non-control temperatures were equally represented in any given session, these were sampled without replacement and interspersed with control blocks.

Behavioral data was labelled by temperature and the analysis mainly consisted in comparing the differences across the four different temperature groups. The number of manipulation sessions performed with each animal was different: Alan has data from 4 manipulation sessions, Joey from 3 and Chandler from 8. Moreover, for the above-mentioned reasons (section 4.1), all data acquired during Roger's manipulation sessions was not considered for the analyses presented henceforth. Finally, there were trials systematically associated with longer reaction and movement times as well as chance-level performance, that were suggestive of disengagement. For this reason, these spurious trials were considered as outliers, as they did not necessarily reflect time judgments. An outlier was defined as a trial with a reaction or movement time above the 95 % percentile or with reaction times below 30 ms (as motor responses to an auditory queue are not expected to be faster than 50 ms), and were excluded in further analysis.

After dividing the data collected over all manipulation sessions by temperature, we pooled together data from all sessions for each individual animal and analysed the corresponding discrimination behavior using the psychometric function described on equation 3.1 introduced in section 3.7 (figure 4.6). This provided us with readily interpretable parameters that we could use to better quantify and visualize the effects of our manipulation.

Consistent with the hypothesis that cooling down striatal tissue would lead to slower dynamics, which would in turn lead to a lower propensity for long judgments, two out of the three animals exhibited a dose-

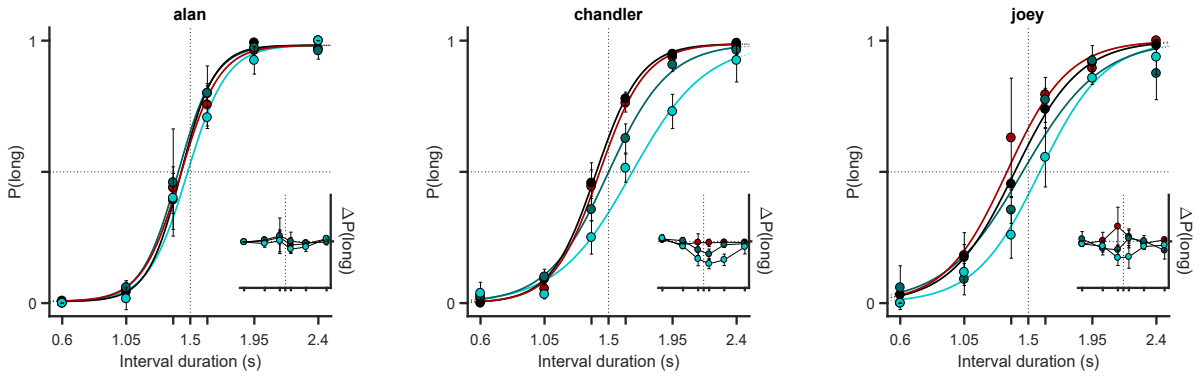

Figure 4.6: Discrimination behavior of individual animals across all manipulation sessions. Psychometric curves for each temperature dose for all sessions of each individual animal (mean ± s.e.m across sessions and psychometric fits; Alan: n = 4; Chandler: n = 8; Joey: n = 3). Red, black, teal and cyan correspond to blocks in which the lower plate of the peltier device was set to 42, 36, 25 and 15 ^{o}C, respectively. The color scheme is preserved in all figures of this section. The insets in each panel correspond to the difference of the long choice proportions between manipulation and control temperatures for each interval duration (mean ± subtraction displacement).

dependent decrease in the proportion of long choices for cold manipulation temperatures, whereas one (Alan) only did so for the coldest temperature (figure 4.6). Systematic stimulus-dependent but category-independent biases towards the short choice port were captured by a rightwards shift in the psychometric curve, which corresponds to an additive change in discrimination threshold.

To better visualize the effects of our manipulation and increase the confidence in our psychometric curve estimates, we pooled data from all sessions and from all three animals, plotting again for each temperature the probability of categorizing a given stimulus as long as a function of the presented interval duration (figure 4.7, left).

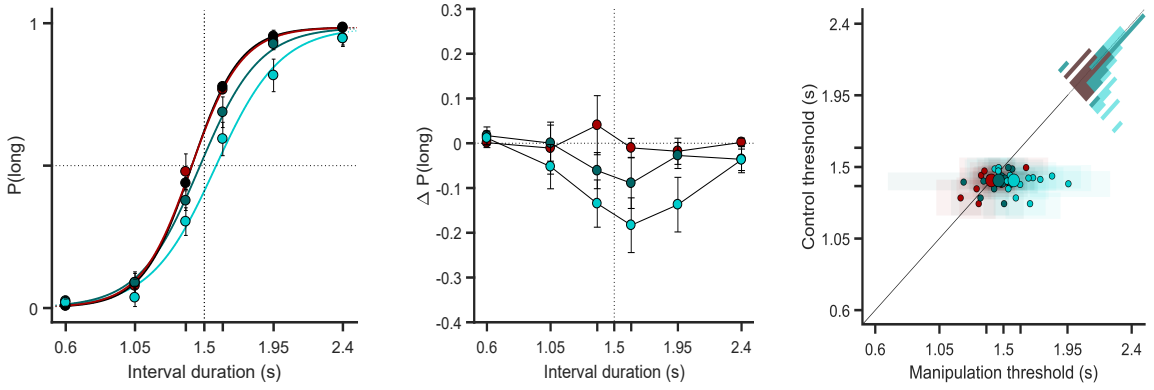

Figure 4.7: Temperature manipulations caused dose-dependent changes in duration judgments. Discrimination behavior for each temperature condition across all manipulation sessions (mean ± s.e.m and psychometric fits, n = 15, **left**). Difference between long choice proportions in manipulation and control temperatures for each interval duration (mean ± subtraction displacement, **middle**). Thresholds of the psychometric fits for each manipulation dose as a function of the corresponding control threshold. Small markers correspond to the maximum-a-posteriori (MAP) for single sessions. Big markers correspond to the thresholds for the fits with sessions pooled together and for each manipulation dose plotted as a function of the corresponding threshold of the psychometrics fit for the control blocks of all sessions. Histograms on the diagonal show the distributions of Δ threshold (manipulation - control) for individual sessions. Color patches represent 95 % of confidence intervals for MAP estimates **(right)**.

At this point we were convinced of the dose-dependency in our cooling manipulations, but were less so regarding the bidirectionality of the effect. We had yet to observe consistent and substantial biases towards the long port on the warm condition so as to be captured by the psychophysical parameters of interest in our psychometric model (threshold and width). However, by pooling more data together, it can be seen that for a given stimulus, namely the near boundary stimuli, long choice proportions seem to be ordered according to temperature, as trials from higher temperature blocks have a larger proportion of long choices than trials corresponding to lower temperature blocks. This ordinal relationship in temperature-specific probabilities of choosing the long port (from the coldest to the warmest temperature) hinted that our manipulation may indeed be inducing bidirectional changes in animals' discrimination behavior.

For a more comprehensible visualization of these changes, we plotted the differences between long choice proportions in manipulation temperatures and the control temperature (ΔP(long)), for all six stimuli (figure 4.7, middle). Again, we see a prominent difference between cold manipulation temperatures (25 and 15 ^{o}C) and control, especially in near-boundary stimuli. However, the differences between the 42 ^{o}C temperature blocks and the control only seem to be evident in one of the near-boundary stimuli. If we had stopped analysing data at this point, we might have convinced ourselves that warming striatal tissue did not induce the systematic behavioral changes that in the context of our the task would translate into a leftwards shift in the psychometric curve.

This suggested shift is essentially captured by one parameter of the psychometric function: the threshold. This parameter is mathematically defined as $S_{0.5}^{-1}$ (see equation 3.2), the inverse of the unscaled sigmoid at chance level performance. As such, a rightward (leftward) shift in the psychometric function corresponds to an increase (decrease) in the point of subjective equality (Wichmann and Hill, 2001). The rightmost plot of figure 4.7 relates thresholds fitted with data from manipulation temperatures of all sessions and their respective control counterparts. This scatter plot speaks to the robustness of the dose-dependent effect summarized in its accompanying panels (figure 4.7), with cold temperature data points below the unity line and the warm temperature slightly above unity. However, it also highlights that there is non-negligible variability across sessions.

Although the differences in fits for the control temperature and manipulation temperature of 42 ^{o}C seem to be negligible, this information does not seem to be coherent with the data collected for one of the two near boundary stimuli (1.38 s). The inconsistency in these analyses rose the question: is it possible that there is a behavioral effect induced by the 42 ^{o}C manipulation dose but it is being masked by undercover effects that we are not taking into account? Indeed, effects such as the homoeostatic mechanisms that compensate temperature in a homeothermic animal or behavioral adaptation to the task across sessions, that has been noticed in pilot experiments done in the lab, could be affecting the efficiency of temperature manipulations in the brain tissue, especially in temperatures closer to the control temperature.

We noticed that in the first manipulation session (figure 4.8, top), the previously observed tendency for a higher propensity to choose long in manipulation blocks with a higher temperature, especially in near boundary stimuli, was maximally observed for all three animals. In fact, this consistent temperature-

dependant behavior across all three animals is even more remarkable on their first sessions when compared to the data pooled from all sessions. However, as more data from manipulation sessions was collected, it was noticed that the conspicuous sequential shift between the four psychometric curves on the first session seemed to become more subtle session after session, as the curves became practically overlapped and indistinguishable, up to a point where the dose dependent behavior is completely lost (figure 4.8, bottom). This effect is especially pronounced when considering evolution of the psychometric curve of the coolest temperature (cyan blue) over sessions in comparison to the control psychometric fit on the same session.

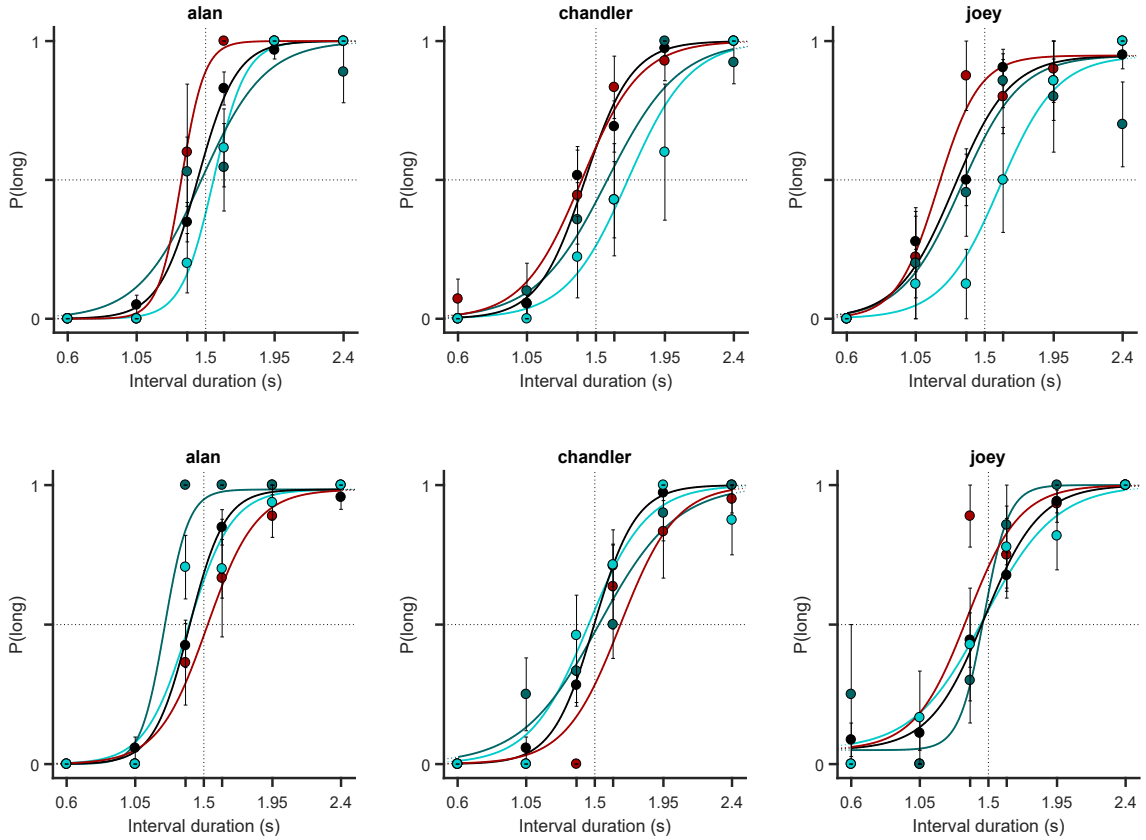

Figure 4.8: Manipulation effect on behavior changed from the first to the last manipulation session. Psychometric curves for each temperature dose for the first **(top)** and last (**bottom**) manipulation session of each individual animal (mean $\pm$ s.e.m across sessions and psychometric fits).

As it was previously mentioned, this decrease in the magnitude of the manipulation effect through sessions has been observed before in pilot experiments done in the lab. In fact, this observation was the main reason why we decided to incorporate interleaved washout sessions in our protocol. This was done to counter any adaptive strategy that animals might have developed during manipulation sessions, that would ultimately mask their effect. This gradual decrease in the magnitude of the manipulation effect could be possibly explained by several variables such as tissue scarring around the implanted probes that changes the tissue's thermal properties or by the development of an adaptation mechanism by the animals over sessions. This eventual adaptation mechanism could allow animals to correct their behavior within a manipulation block, as they receive feedback from their performance after each trial.

To ascertain these trend, we decided to look into the into non-stationary effects over manipulation

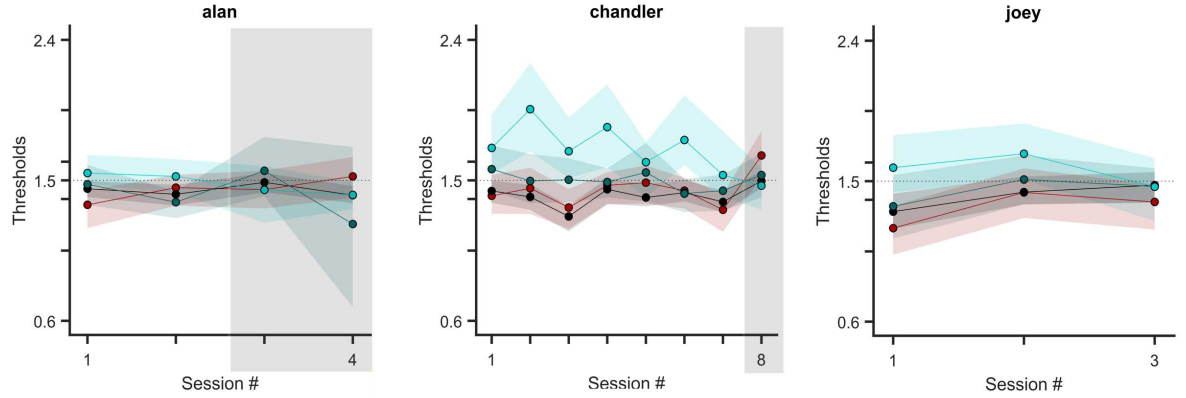

Figure 4.9: Magnitude of the temperature effect size progressively dwindled across session. Threshold of the psychometric fits for each temperature dose for each manipulation session (with 95% confidence intervals represented by the color patches). Grey rectangles are surrounding manipulation sessions wherein the most extreme manipulation dose (T = 15 ºC) is no longer producing an effect. These highlighted manipulation sessions were excluded in further analysis (see text).

sessions by analysing the threshold values of the psychometric curves over sessions (figure 4.9).

On the first session, the inverse relation between temperature and threshold value discussed above is seen for all animals except Joey, where these values for the control temperature and 25 ^{o}C are swapped. As one looks into the number of sessions axis, it can be seen that this relation and order between temperatures smears out to a point where this pattern is not always clear between the 25 ^{o}C and the 42 ^{o}C data points. For all animals, the plots for the cooling temperatures (cyan blue and tile) show a peak at a given session, after which threshold values tend to converge to the threshold value of the control blocks. The same happens in the plots describing threshold variation over sessions on warming blocks (red) but instead of a peak, a trough is observed.

In these plots figure 4.9 can further be seen that it takes a smaller number of sessions for the threshold values of 42 ^{o}C and 25 ^{o}C blocks to converge to the control block thresholds than for the coolest temperature blocks (15 ^{o}C). This suggests a faster adaptation of the animals to these manipulation doses that could be contributing for similar curve fitting between these temperatures and the control shown in figure 4.7.

However, after a certain number of manipulation sessions (Alan - 4 sessions; Chandler - 8 sessions; Joey - 3 sessions), the inverse order of the threshold values with temperature disappears, even for the coldest and farthest from the control temperature, up to a point where the temperature effect is inverted.

Following this idea of animals adapting their behaviour to the temperature manipulations, it is reasonable to hypothesize that adaptations may be occurring at other times scales. We saw in figure 4.9 the shift between the psychometric curves of different manipulation temperatures disappearing over sessions, as the differences between manipulation and control data smeared, but would the animals be able to adjust their behaviour during 3-minutes manipulation blocks? Indeed, periods before and after block transitions can be considered less stable than periods in the middle of a block. The first thing to consider should be that temperature changes are not done instantaneously: not only does the temperature of the cold plate of the peltier only reaches the set temperature after a 3 second step time to

avoid overshoots that may damage the brain, but also it needs to be considered a period of time for the striatal tissue change its temperature. Furthermore, there can be other effects occurring within these transition periods that may be affecting the temperature manipulations during a block. On one hand as one gets closer to the ending of a temperature manipulation block, by developing an adaptation mechanism, animals can be correcting their behavior via feedback in order to make a correct choice and to be rewarded. Moreover, tissue homoeostasis in mammals can be contributing to counter the manipulation effect by trying to reestablish the biological temperature of the brain. On the other hand, at the beginning of control blocks after a transition from a manipulation block, the striatal tissue can be still recovering from the manipulation temperature at different time rates. Hence, these ”leakage” temperature effects may be affecting the animals' behavior at the beginning of control blocks.

To address this question, we looked at the variation of the thresholds for each dose across block transitions (figure 4.10). For this purpose, we defined a time window with half of a block length and looked at thresholds from psychometric curves defined by trials made during a time window, which then we slide in a way that included the next 5% of the block length, allowing to calculate a new threshold value.

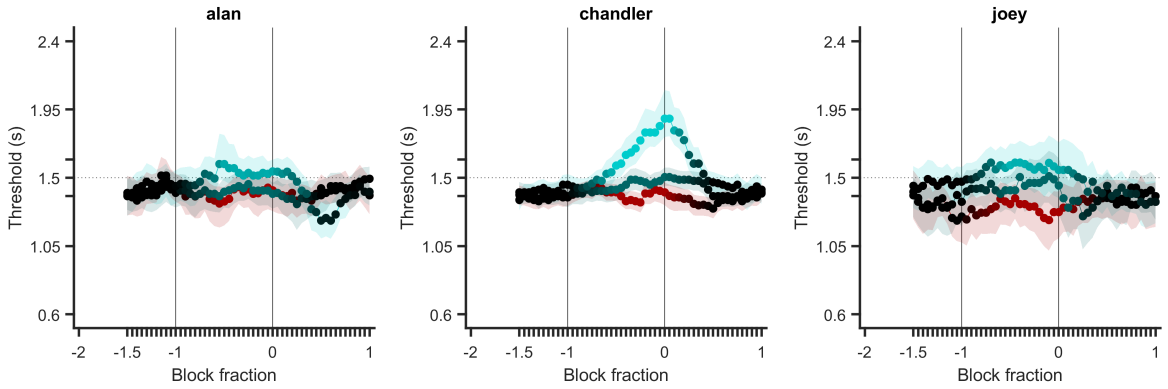

Figure 4.10: Magnitude of manipulation effects is nonstationary within blocks. Thresholds of psychometric fits calculated within 95-s wide, 9.5-s apart, overlapping time windows. These correspond to 50 % and 5 % of block duration, respectively. For each manipulation temperature, we applied this sweeping procedure starting from the beginning of the preceding control block until the end of subsequent one. Manipulation blocks are comprised between block fractions -1 and 0 and the following control blocks between 0 and 1. Colors grade from dark to the light color of each manipulation block according to the fraction of control blocks included within a time window (100 % for black circles and 0 % for pure and bright colors).

During manipulation blocks (block fraction comprised between -1 and 0), animals seem to display very different behaviors. For both coldest and warmest doses, in Alan's data there seems to be a peak and a through, respectively, around half the time of a manipulation block. Similarly to Alan, Joey's data also follows this tendency, however, by the end of a manipulation block, the doses seem to be separating from the control threshold again and in the ordered direction, suggesting that the manipulation effect is reappearing by the end of the manipulation block. Finally, Chandler's data suggests that the effect of manipulations is maximal late in a block, as differences between doses' thresholds are more accentuated by the end of a block. Therefore, although the variations of the manipulation effect are not consistent across animals, middle portions of the blocks always register a clear difference between doses and

between the control temperature.

Despite the inconsistency in the magnitude of the effect within a manipulation block, data from control blocks seems to be consistent across animals, showing that the threshold value converges again to the control value around half of the time of a control block.

For a better understanding of the effect of manipulating striatal tissue with temperature, we arbitrated that only data acquired until the session wherein the most extreme manipulation dose produced an effect (T = 15 ^{o}C) would be considered for further analysis, i.e., until the last session where the highest threshold values were registered for the 15 ^{o}C data. Our criteria was based on the coldest temperature data since this was the temperature showing the most consistent effect across sessions. Therefore, if the effect was no longer present when using this temperature, it was likely not to be present in any other manipulation temperature (with a smaller dynamic range) from the set. By establishing this threshold, the total number of manipulation sessions further considered in the results is 12 (Alan - 2 sessions; Chandler - 7 sessions; Joey - 3 sessions). Moreover, due to the several possible non-stationary events occurring near block transitions, we also decided to take a closer look to data comprised between 10 and 75 % of the block length of manipulation blocks as well as the latter half of the control blocks.

We then pooled these selected data together and analysed the overall temperature effect on these 12 manipulation sessions with 5485 trials: 794, 978, 2791 and 922 trials for 15 ^{o}C, 25^{o}C, 36 ^{o}C and 42 ^{o}C, respectively (figure 4.11). Again, we used the curve fitting described in equation 3.1 to fit a psychometric curve to the data points of the control temperature blocks and compared data from different manipulation temperatures and the control.

When taking into account eventual behavioral adaptations, it becomes clearer that all manipulation doses seem to be causing a behavioral effect considerably different from the control, as there is a remarkable distinction between the fittings of all four-conditions psychometric curve (figure 4.11). The change in the threshold of the fittings for each temperature visually stands out as a shift between the psychometric curves: the coldest the temperature, the more shifted to the right is the psychometric curve (figure 4.11, bottom left). These shifts in the psychometric curves are even more emphasized when plotting the differences between the data points of manipulation and control temperatures (ΔP(long) - figure 4.11, top right), with negative values for the colder than control temperatures and positive values for the warmer temperature, meaning that the probability of reporting a stimulus as long is smaller/bigger for colder/warmer temperatures than control, respectively and especially for near boundary stimuli.

Furthermore, we plotted the probability density functions of the psychophysical parameters that describe the fitting curves for each temperature block (figure 4.11, bottom right). These plots add further support for a dose dependent behavior in the context of the task by showing that the changes in manipulation temperature data from all sessions of all three animals seem to be explained with a change in the psychophysical parameters that set the threshold and the width of the sigmoids.

Ultimately, this ordered shift between different psychometric curves suggests that the categorical boundary of the animals while solving the task is being shifted by temperature: by being more (less) likely to judge a stimuli as long during a warmer (colder) than control temperature, the categorical boundary during these blocks becomes shorter (longer) than 1.5 seconds, thus being shifted to the left (right) in

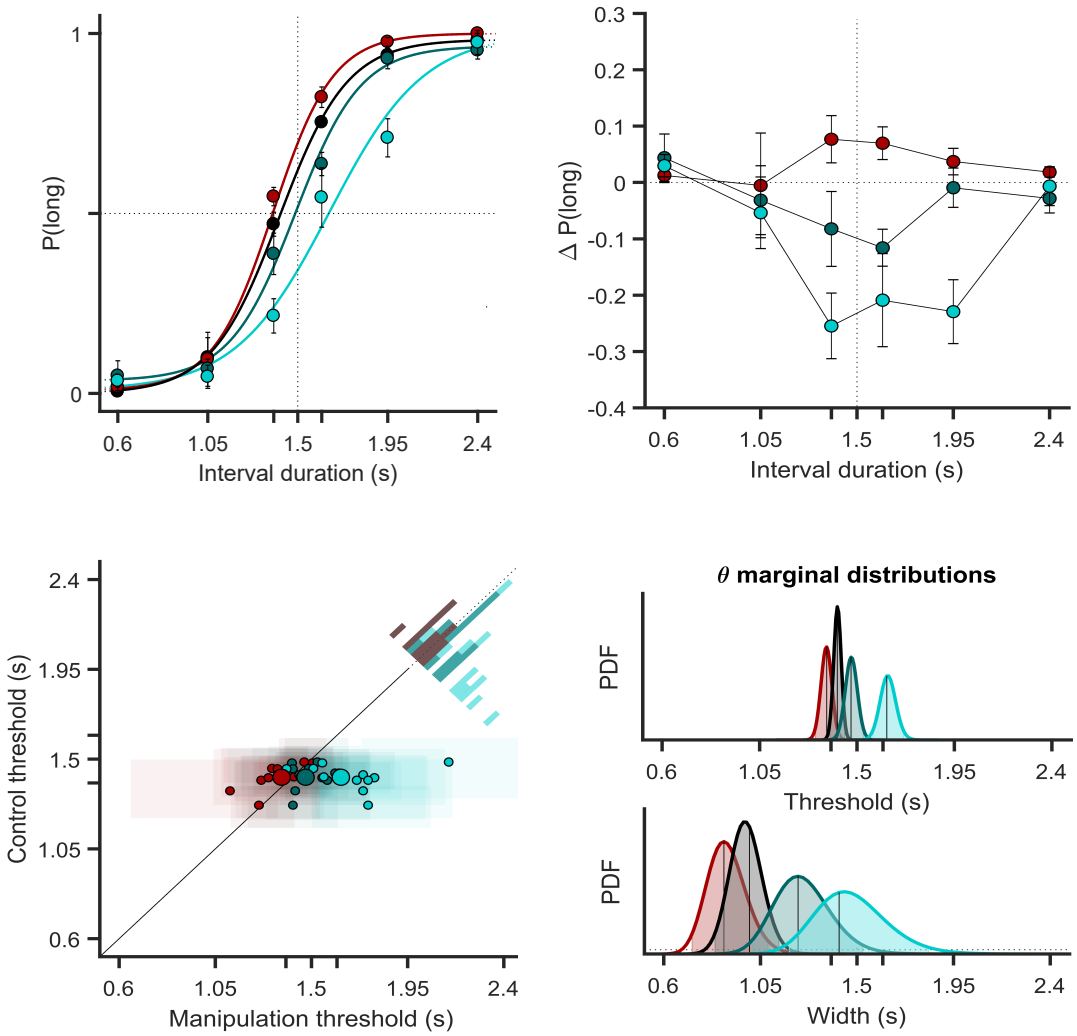

Figure 4.11: Changes in striatal temperature caused bidirectional and graded changes in estimates of elapsed time. Discrimination behavior for each temperature condition across all manipulation sessions (mean ± s.e.m and psychometric fits, **top left**). Difference between long choice proportions in manipulation and control temperatures for each interval duration (mean ± subtraction displacement, **top right**). Thresholds of the psychometric fits for each manipulation dose as a function of the corresponding control threshold. Small markers correspond to the maximum-a-posteriori (MAP) for single sessions. Big markers correspond to the thresholds for the fits with sessions pooled together and for each manipulation dose plotted as a function of the corresponding threshold of the psychometrics fit for the control blocks of all sessions. Histograms on the diagonal show the distributions of Δ threshold (manipulation - control) for individual sessions. Color patches represent 95 % of confidence intervals for MAP estimates **(bottom left)**. Probability density functions of the parameters defining the logistic function - threshold (top) and width (bottom) - in the psychometric fits for each temperature. Vertical lines correspond to the MAP estimates shown in the top left panel **(bottom right)**.

the time axis.

Since the manipulations were being made in a basal ganglia nuclei (i.e., striatum), which is highly involved in motor responses, we wanted to check if animals' motor behavior was also being affected. For that purpose, apart from the performance of the animals in the timing task, we also looked at the influence of different temperatures in reaction and movement times. Figure 4.12 depicts the reaction and movement times for each temperature manipulation as a function of the trial stimulus.

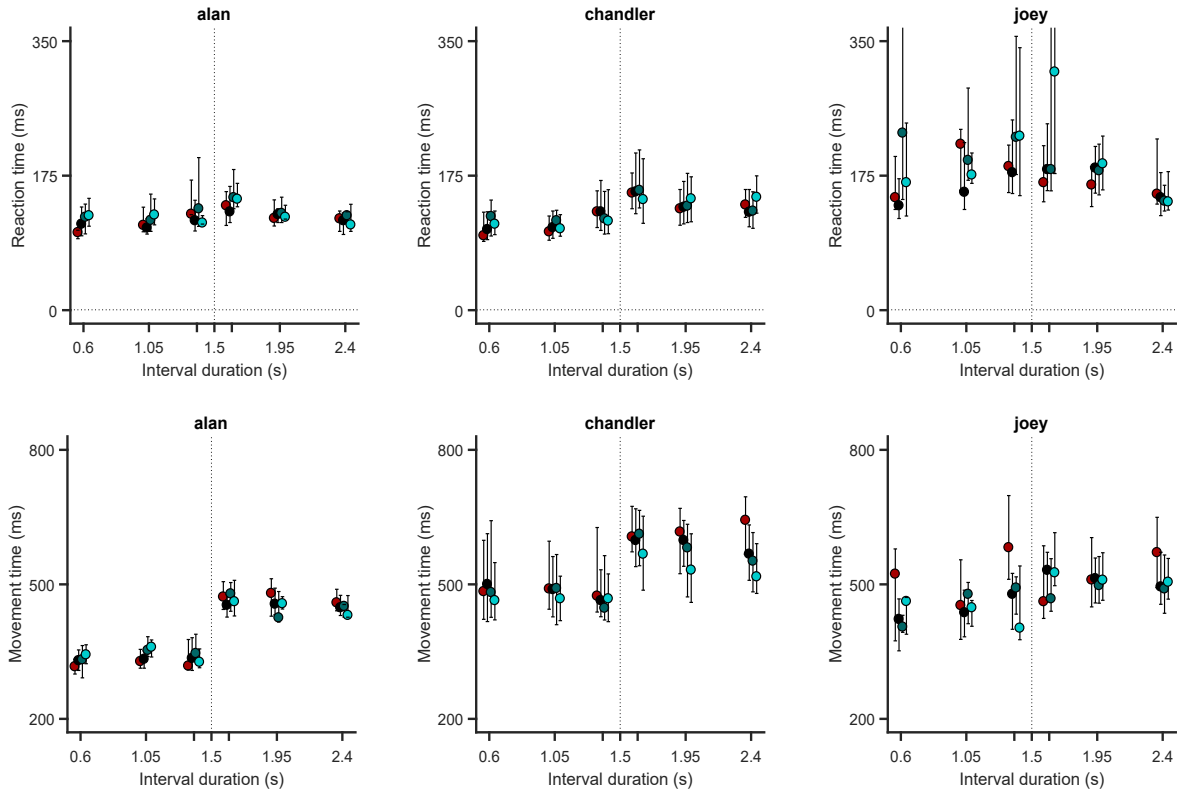

Figure 4.12: Animals' motor responses were not affected by changes in the striatal temperature. Average reaction (top panels) and movement (bottom panels) times for correct trials for every temperature dose and for each individual animal (median $\pm$ interquartile range, Alan: n = 2 sessions; Chandler: n = 7 sessions; Joey: n = 3 sessions).

For all animals and for each one of the stimulus individually (except for one near boundary stimuli in Joey's data), it is consistently observed that there are no abrupt changes in the reaction times with the manipulation temperature of a block. The same independence from temperature can be seen in the plots describing movement time as a function of the stimulus. However, in these plots it can be noticed that longer stimuli (or movements to the left side) are often associated with slower movement times than shorter stimuli/movements to the right.

Taken together, these data show that there are no evident motor effects of temperature while performing the task, suggesting that the rats' motor activity, unlike a cognitive variable such as time judgment, is not being affected by temperature.

All in all, the presented results provide evidence of a causal relation between the speed of striatal population and timing judgments, being strongly congruent with early work done in the lab showing that speed of population activity run faster or slower when animals judge a given stimulus as long or short, respectively (Gouvêa et al., 2015).

4.4 MRI

After being sacrificed, animals' brains were collected and the placement of the implant silver probes was confirmed with MRI.

From MRI coronal slices, we identified the lesions' location for each animal and determined its intermediate (anterior-posterior, AP) slice (figure 4.13). It can be seen that the placement of the probes was not completely parallel, as one probe is more ventrally placed than the other, especially when considering the slices of Alan and Joey. To maintain a parallel configuration of the probe during the surgical placement of the implant is very difficult due to silver's relatively reduced stiffness. Additionally, a slight pushing movement during the extraction of the implant or any brain deformation during the extraction of the brain could also have contributed to the asymmetries of the implant placement observed in the images. Furthermore, when comparing the scanning of Alan with the other two animals, there are salient differences in the quality of the acquired images. These differences are likely due to the fact that both Chandler and Joey were perfused (see section 3.8), contrarily to Alan, who died unexpectedly during the experiments. Since the perfusion procedure contributes to a better fixation and preservation of biological tissues, it was expected that skipping this critical step in the preparation of imaging would result in a loss of imaging quality of the slices.

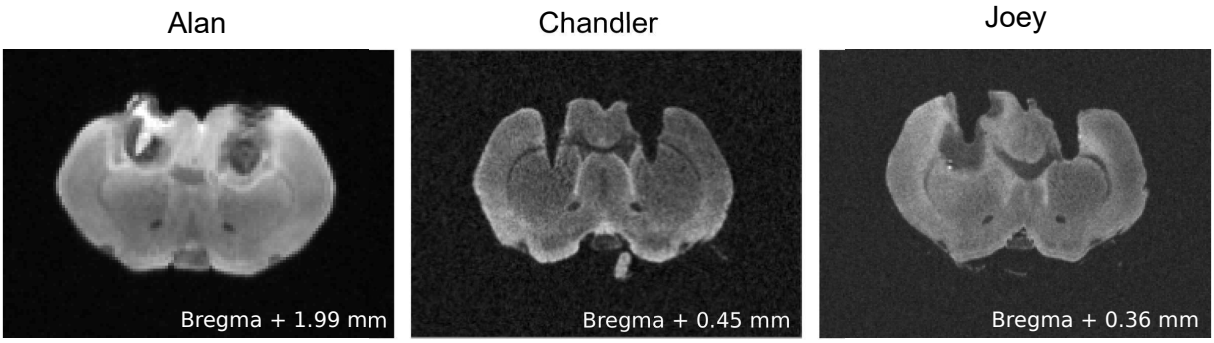

Figure 4.13: Implant probes were successfully placed in the dorsal-central striatum of all three animals. Coronal MRI scanning of the middle lesion slices for each one of the animals. The estimated AP distance from Bregma, calculated comparing with a reference slice from an atlas (Paxinos and Watson, 2006), is in the bottom right corner of each image (spatial resolution of the scanning: 150 x 150 x 150 μm^3).

To estimate the position of the implant, we also matched each reference slice with the corresponding one from a rat brain atlas in stereotaxic coordinates (Paxinos and Watson, 2006). By knowing the AP location from Bregma of the reference slice (given by the atlas) and knowing that the spacing between consecutive coronal slices is 150 μm, we were able to estimate the AP distance from Bregma of the middle lesion slice and compare it with our target value (+0.84 mm AP from Bregma).

With these estimations, even though the probes are not perfectly placed in parallel, it can be seen that the striatum was successfully targeted in all three animals.

Overall, the confirmation of a correct placement of the implant allowed us to more confidently affirm that striatal temperature was indeed being manipulated, inducing changes in animals' duration judgments in the context of the task.

Chapter 5

Conclusions

5.1 Discussion

We trained rats in an interval categorization task to analyse changes in their time judgment induced by temperature manipulations of the striatal tissue.

A structured and detailed planning of several stages allowed a progressive training of the behavioral paradigm to the animals, gradually introducing them to the final timing task. Roughly after two months since the beginning of training, all animals displayed a very reliable time sensitive behavior, being able to consistently categorize correctly the intervals with a performance above 70%. Nevertheless, we believe that the training duration could be shortened if the sessions were done uninterruptedly (7 days a week), as we noticed that performance seemed to drop persistently on every session after the two days of pause.

We consider that this close and systematic monitoring of the training sessions (as well as the animals' well being and experimental setup conditions) from the first day of training up until the period after surgery recovery was a crucial process as it led to the development of a highly consistent behavior and performance across animals in the task. Therefore, this reproducibility allowed a reliable inter-animal comparison on their behavior and on the effects of temperature manipulations.

Another fundamental step in this study was the successful design, characterization and validation of our custom-made thermoelectric implant. The implant developed was capable of stably operating during the three minute period of each manipulation block within a broad range of temperatures, that included the values used for the manipulations. The range of these values was defined so that no thermal damage in the neural tissue was induced, taking into account that spiking activity is blocked below 10 ^{o}C (Brooks, 1983) and that temperatures above 43 ^{o}C cause damage in the structure of proteins (Katschinski, 2004). For these reasons, stability at the set temperature was a key feature achieved in the engineering of the implant, being the measured fluctuations in the order of the 0.1 ^{o}C. Indeed, in pilot experiments stability around a set temperature was not being achieved due to overheating of the top plate of the implant, as the heat dissipation rate, being passive, was not fast enough. However, by introducing an active heatsink to the implant this stability feature was guaranteed, further allowing us

to do a dose-dependent manipulation and not only a single cooling condition, as done before in pilot studies from the lab. Moreover, having an implant that does not overheat during a manipulation block reduces the possibility of this sensory variable queuing the animals of block transitions, potentiating faster adaptation to the task. Still considering the narrow temperature range in which the animals' health is not compromised, another important adjustment was at the control level of the implants by finding a trade-off between the speed of block transitions and the avoidance of over or undershoots to biologically-threatening temperatures.

Since the striatum, the region of interest of this study, is located deep in the brain, a thermally conductive probe had to be attached to the lower plate of the thermoelectric device to allow heat transfer (Aronov and Fee, 2011). When characterizing the implant in warmed agarose (2% V/V), which mimics the brain tissue thermal properties (Kim et al., 2007), despite the use of a highly thermal conductive material for the probes and poor thermal conductive insulation materials up to the tips, we registered an offset between the set temperature at the lower plate and the temperature at the probes' tip. These registered differences were not surprising since the materials of both insulation and conduction are not perfect. Furthermore, this *in vitro* characterization of the implant is also lacking the consideration of natural biological thermoregulation mechanisms that seek to maintain the temperature homoeostasis of homoeothermic animals (Bligh, 1966). Nevertheless, defining a function of the temperature at the tips according to the set temperature at the lower plate of the TEC device was an important step towards choosing with more principled and objective criteria the temperature doses used in the manipulation sessions.

The results from the MRI scannings show that, in all surgeries, the implants were placed in the dorsal-central striatum, successfully targeting a brain area previously implicated in timing (Gouvêa et al., 2015). This post-*mortem* confirmation of the probes' placement shows that the temperature manipulations should be affecting the dorsal-central striatum, despite not having a defined function describing a quantitative measurement of the decay of temperature with the distance to the tip of the probe.

Overall, these results describing animals behavior during all training stages and implant development and placement constitute the main technical requirements that we needed to develop to reach the main purpose of this project: to analyse animals' behavior in the context of our timing task while manipulating the temperature of striatal tissue.

Our findings show strong evidence of a causal and dose dependent and bidirectional relation between the speed of striatal population dynamics and the animals' judgment of elapsed time. Agreeing with our hypothesis that cooling down striatal tissue would lead to slower dynamics, which would in turn lead to a lower proneness to report long judgments, all animals exhibited a dose-dependent decrease in the proportion of long choices for cold manipulation temperatures and an increase in this same proportion for the warm dose. These proportion differences from manipulation to control temperatures were especially noticed for the two near-boundary stimuli, which were the most difficult to correctly categorize. The systematic stimulus-dependent but category-independent biases towards the short (long) choice port were captured by a rightwards (leftwards) shift in the psychometric curve, corresponding to a change in the animals' discrimination threshold. However, given the cumulative nature of the decision

variable in our task and the posited effect of our manipulation on the speed of striatal dynamics, an asymmetric impact on reports regarding stimuli on both sides of the boundary was also to be expected and observed. This stimulus-proportional bias can be interpreted as a decrease in timing sensitivity and modelled as an increase in width (decrease in slope) in the chosen psychometric function to fit the data.

However, the bidirectonality of the manipulation effect only became evident and consistent for all animals after considering the influence of several undercover mechanisms that could be masking the effect of temperature manipulations.

Besides the highlighting of a non-negligible variability across sessions registered in our data, data collected during an earlier pilot experiment in the lab, wherein only one cold temperature value was used, showed that the size of the manipulation tended to be maximal on the first manipulation session and gradually decreased across the following. This tendency was the foremost reason why we decided to incorporate interspersed washout sessions into the experimental protocol, in hopes to counter adaptive strategies that animals might have been developing during manipulation sessions, that could ultimately hide their effect. Despite this added control, the effect of the manipulations on the animals' behavior faded away, with the number of sessions with a consistent effect being variable across animals. Therefore, pooling data over sessions indiscriminately like we did on a first analysis led to a misestimation of the magnitude of the effect.

This project does not allow us to find a definite explanation for these observations, the gradual decrease in the magnitude of the manipulation effect could be due several different variables. From an engineering perspective, it could be assumed that the TEC device of the implant could have a drop of performance with time. Consequently, the manipulation temperatures on the first session would not be the same as the ones on latter session, as the performance of the device in reaching the set temperature decreased from session to session. However, we registered similar performances of the implants before and after the experiments, giving us more confidence to rule out a malfunction of decrease in the devices' performance across sessions as one of the explanations for the decrease in the magnitude of the effect.

Another explanation could be the post-surgery development of glial scarring around the implanted probes, reported several times in electrophysiological studies (Griffith and Humphrey, 2006). The growth of glial elements on the implant likely changes its impedance and resistance with time after implantation, potentially affecting the probes' performance. Nevertheless, since manipulation sessions started three weeks after implantation and were done every other day over a period of two weeks, all sessions should have been affected by gliosis around the chronic implant roughly the same way. Therefore, it is very unlikely that glial scarring fully captures the variability between sessions that we observed.

A third and more presumable explanation relies on the development of an behavioral adaptation mechanism by the animals over sessions. Since animals received feedback for every choice made, the period within a block can be sufficient for an adaptive strategy to emerge. Therefore, it is reasonable to posit that session after session this period decreases, allowing animals to correct their behavior at an earlier stage, decreasing the effect of the manipulations.

After considering compensatory mechanisms interfering with the effect, both within manipulation and

control blocks and across sessions, the dose-dependency and bidirectionality of the effect becomes remarkably evident. The differences between doses captured by the psychophysical parameters of our fits (threshold and width) show compelling evidence supporting that temperature changes in the striatal tissue, hence in its circuit dynamics, induce changes in the animals judgment of time in the context of the behavioral task.

Despite several lines of evidence showing its involvement in timing (Maricq and Church, 1983; Hinton and Meck, 2004; Meck, 2006; Gouvêa et al., 2015), the basal ganglia is a crucial structure in the control of movement (Gerfen and Bolam, 2010). Therefore, temperature manipulations within this brain region could have been inducing changes in the animals' motor responses, with cooling slowing down movement, and warming, which should speed up movements. However, both reaction and movement times show no substantial changes between different temperatures and for all animals tested.

Intriguingly, it seems that there is a tendency for longer movement times for intervals longer than the categorical boundary. In this work, as in many decision-making paradigms, categorical judgments (e.g., long/short) are reported through lateralized movements (left/right), being this rule fixed. To be able to distinguish these variables, the choice sides could have been switched so that long choices would be reported on the right port and short choices on the left one. However, previous experiments from the lab have shown that it is not trivial to train contingency reversal in this task.

In conclusion, our study shows that although manipulations of striatal temperature were inducing bidirectional dose-dependent changes in the animals' time judgments, they were not affecting any motor responses. Our data provide strong support for the hypothesis that the brain derives estimates of elapsed time from population dynamics. Moreover, we showed compelling evidence that the BG are not only implicated in the control of movement, being also a crucial structure for encoding cognitive variables such as elapsed time.

5.2 Future Work

This study has been able to corroborate previous studies done in the laboratory, showing a causality between the speed of striatal dynamics and animals' judgment of the elapsed time. Nevertheless, several improvements to our study as well as future experiments are needed to gain further insights into this relation.

From a more technical point of view, additional work could be useful in both modelling and experimentally quantifying the thermal propagation in the brain. Knowing the decaying relationship between the temperature and the radial distance from the tip of the probe would allow us to have more information about the volume of tissue being affected by the manipulations. Moreover, quantifying this decay along the probe axis (from the lower plate to the tip) would allow us to analyse the efficiency of our insulation strategy and to verify that cortical areas crossed by the probe were not being strongly affected by the temperature manipulations.

Regarding complementary experimental work, there are several additional experiments that could be done with the purpose of explaining some questions that this project rose. Firstly, we plan to run more

animals in this exact same experimental paradigm to collect more data, hence gaining more confidence and statistical power in our results. Furthermore, more data could allow us to take a closer look to the adaptation mechanisms developing during manipulation and control blocks. In this work, we hypothesised and arbitrated that the manipulation's effect would be maximal on the first and latter portions of manipulation and control blocks, respectively. However, by analysing thresholds' variation that define the psychometric curves within a block, we would have a more principled way of selecting data. Moreover, the selection and exclusion of outlier trials could have been more strictly defined, for example in a data-driven way instead of manually coded.

To address the question of animals adapting their behavior across sessions as a function of the feedback they receive, non-implanted animals could be tested in the same timing task where the categorical boundary is changing in blocks with the same duration as in the temperature manipulation blocks. Consequently, control blocks, in which the categorical boundary is set at 1.5 s, would be interleaved with two different types of manipulation blocks: blocks in which the categorical boundary is shifted towards longer or shorter than 1.5 s duration times. Under the longer than 1.5 s boundary scenario a near-boundary stimulus (1.62 s) should be reported as short, while in shorter than 1.5 s boundary blocks near-boundary stimulus (1.38 s) is only correctly categorized if animals report a long choice. If animals can correct their behavior to this paradigm over sessions, these experiments would provide strong evidence for the development of an adaptation strategy that can justify the decreased effect of the temperature manipulations observed in our results.

Ultimately, the ideal experiment would be to simultaneously perform temperature manipulations and recordings of neural activity in behaving animals, confirming that indeed cooling and warming of the striatal tissue is slowing down and speeding up the circuit dynamics in the context of our task, respectively. However, the combination of temperature and activity measurements are not easy to perform (Girardin and Martin, 2009) and would have been really difficult to achieve within a six-months project, as is the case of the work presented in this dissertation.

5.3 Personal Remarks

These last six months working at the Champalimaud's Learning Laboratory were by far the most enriching experience I have had over my five year academic path.

The opportunity of integrating such an incredible scientific community allowed me to be exposed to the daily challenges but also excitement of learning and doing science. From the long and intense discussions of data and recent papers during lab meetings to the weekly internal seminars and colloquia, in which people from the inside and outside of the foundation give a presentation about their work, I got to hear and question some of the most interesting studies that have been recently done in neuroscience.

Moreover, during this semester I was given the opportunity to develop important skills in neuroscience by attending to a practical and theoretical course on laboratory animal science as well as to a training in microscopy. Apart from these courses, the daily work at the lab allowed me to improve not only to programming and engineering skills but also to enhance my ability to talk and to write in a clearer and

more objective way, which are crucial to communication in science.

My stay at the the lab culminated with the opportunity of attending and presenting a poster at this year's Champalimaud Research Symposium on quantitative approaches to behaviour & neural systems, where I was able to get in touch with so many different projects and people from all around the world.

Being part of this project, and more generally of the Champalimaud Foundation, allowed me widen my horizons and to grow both personally and professionally. I am excited and looking forward to proceed a path in neuroscience and hopefully give my contribution back to investigation in this field.

Bibliography

Albin, R. L., Young, A. B., and Penney, J. B. (1989). The functional anatomy of basal ganglia disorders. *Trends in neurosciences*, 12(10):366–375.

Alexander, G. E., DeLong, M. R., and Strick, P. L. (1986). Parallel organization of functionally segregated circuits linking basal ganglia and cortex. *Annual review of neuroscience*, 9(1):357–381.

Aronov, D. and Fee, M. S. (2011). Analyzing the dynamics of brain circuits with temperature: design and implementation of a miniature thermoelectric device. *Journal of neuroscience methods*, 197(1):32–47.

Bell, F. G., Barton, D. K., Laird, J. S., and Jones, C. T. (2003). Digital sensor for miniature medical thermometer, and body temperature monitor. US Patent 6,629,776.

Bell, L. E. (2014). Cooling , Heating , Generating Heat with and Recovering Waste Thermoelectric. *Science*, 321(5895):1457–1461.

Bligh, J. (1966). The thermosensitivity of the hypothalamus and thermoregulation in mammals. *Biological Reviews*, 41(3):317–365.

Braitenberg, V. (1967). Is the cerebellar cortex a biological clock in the millisecond range. *Prog Brain Res*, 25:334–346.

Broca, P. (1865). Sur le siège de la faculté du langage articulé (15 juin). *Bulletins de la Société Anthropologque de Paris*, 6:377–393.

Brooks, V. B. (1983). Study of brain function by local, reversible cooling. In *Reviews of Physiology, Biochemistry and Pharmacology, Volume 95*, pages 1–109. Springer.

Buhusi, C. V. and Meck, W. H. (2005). What makes us tick? Functional and neural mechanisms of interval timing. *Nature Reviews Neuroscience*, 6(10):755.

Buonomano, D. V. (2007). The biology of time across different scales. *Nature chemical biology*, 3(10):594.

Buonomano, D. V. and Karmarkar, U. R. (2002). Book Review: How Do We Tell Time? *The Neuroscientist*, 8(1):42–51.

Carandini, M. and Churchland, A. K. (2013). Probing perceptual decisions in rodents. *Nature neuroscience*, 16(7):824.

Coull, J. T., Cheng, R.-K., and Meck, W. H. (2011). Neuroanatomical and neurochemical substrates of timing. *Neuropsychopharmacology*, 36(1):3.

Damasio, A. R. (1994). Descartes' error: Emotion, rationality and the human brain.

Fee, M. S. and Long, M. A. (2011). New methods for localizing and manipulating neuronal dynamics in behaving animals. *Current opinion in neurobiology*, 21(5):693–700.

Fenno, L., Yizhar, O., and Deisseroth, K. (2011). The development and application of optogenetics. *Annual review of neuroscience*, 34.

Gerfen, C. R. and Bolam, J. P. (2010). The neuroanatomical organization of the basal ganglia. In *Handbook of Behavioral Neuroscience*, volume 20, pages 3–28. Elsevier.

Gerfen, C. R. and Surmeier, D. J. (2011). Modulation of striatal projection systems by dopamine. *Annual review of neuroscience*, 34:441–466.

Gibbon, J. (1977). Scalar expectancy theory and Weber's law in animal timing. *Psychological review*, 84(3):279.

Girardin, C. and Martin, K. (2009). Cooling in cat visual cortex: stability of orientation selectivity despite changes in responsiveness and spike width. *Neuroscience*, 164(2):777–787.

Gold, J. I. and Shadlen, M. N. (2007). The neural basis of decision making. *Annual review of neuroscience*, 30.

Goldsmid, H. J. (2010). *Introduction to Thermoelectricity*. Springer Berlin Heidelberg, Berlin, Heidelberg.

Gouvêa, T. S., Monteiro, T., Soares, S., Atallah, B. V., and Paton, J. J. (2014). Ongoing behavior predicts perceptual report of interval duration. *Frontiers in Neurorobotics*, 8:10.

Gouvêa, T. S., Monteiro, T., Motiwala, A., Soares, S., Machens, C., and Paton, J. J. (2015). Striatal dynamics explain duration judgments. *eLife*, 4(December2015):1–14.

Griffith, R. W. and Humphrey, D. R. (2006). Long-term gliosis around chronically implanted platinum electrodes in the Rhesus macaque motor cortex. *Neuroscience letters*, 406(1-2):81–86.

Grondin, S. (2010). Timing and time perception: a review of recent behavioral and neuroscience findings and theoretical directions. *Attention, Perception, & Psychophysics*, 72(3):561–582.

Han, Z. and Fina, A. (2010). Thermal conductivity of carbon nanotubes and their polymer nanocomposites: A review. *Progress in Polymer Science*, 36:914–944.

Hinton, S. C. and Meck, W. H. (1997). The 'internal clocks' of circadian and interval timing. *Endeavour*, 21(1):3–8.

Hinton, S. C. and Meck, W. H. (2004). Frontal-striatal circuitry activated by human peak-interval timing in the supra-seconds range. *Cognitive Brain Research*, 21(2):171–182.

Ivry, R. B. and Keele, S. W. (1989). Timing functions of the cerebellum. *Journal of cognitive neuroscience*, 1(2):136–152.

Ivry, R. B. and Schlerf, J. E. (2008). Dedicated and intrinsic models of time perception. *Trends in cognitive sciences*, 12(7):273–280.

Janssen, P. and Shadlen, M. N. (2005). A representation of the hazard rate of elapsed time in macaque area lip. *Nature neuroscience*, 8(2):234.

Jin, D. Z., Fujii, N., and Graybiel, A. M. (2009). Neural representation of time in cortico-basal ganglia circuits. *Proceedings of the National Academy of Sciences*, pages pnas–0909881106.

Katschinski, D. M. (2004). On heat and cells and proteins. *Physiology*, 19(1):11–15.

Kemp, J. M. and Powell, T. P. S. (1971). The termination of fibres from the cerebral cortex and thalamus upon dendritic spines in the caudate nucleus: a study with the Golgi method. *Phil. Trans. R. Soc. Lond. B*, 262(845):429–439.

Killeen, P. R. and Fetterman, J. G. (1988). A behavioral theory of timing. *Psychological review*, 95(2):274.

Kim, J., Ghim, J.-W., Lee, J. H., and Jung, M. W. (2013). Neural correlates of interval timing in rodent prefrontal cortex. *Journal of Neuroscience*, 33(34):13834–13847.

Kim, S., Tathireddy, P., Normann, R. A., and Solzbacher, F. (2007). Thermal impact of an active 3-D microelectrode array implanted in the brain. *IEEE Transactions on Neural Systems and Rehabilitation Engineering*, 15(4):493–501.

Kravitz, A. V., Freeze, B. S., Parker, P. R., Kay, K., Thwin, M. T., Deisseroth, K., and Kreitzer, A. C. (2010). Regulation of parkinsonian motor behaviours by optogenetic control of basal ganglia circuitry. *Nature*, 466(7306):622.

Lapid, E., Ulrich, R., and Rammsayer, T. (2008). On estimating the difference limen in duration discrimination tasks: A comparison of the 2afc and the reminder task. *Perception & psychophysics*, 70(2):291–305.

Leon, M. I. and Shadlen, M. N. (2003). Representation of time by neurons in the posterior parietal cortex of the macaque. *Neuron*, 38(2):317–327.

Long, M. A. and Fee, M. S. (2008). Using temperature to analyse temporal dynamics in the songbird motor pathway. *Nature*, 456(7219):189.

Long, M. A., Katlowitz, K. A., Svirsky, M. A., Clary, R. C., Byun, T. M., Majaj, N., Oya, H., Howard III, M. A., and Greenlee, J. D. (2016). Functional segregation of cortical regions underlying speech timing and articulation. *Neuron*, 89(6):1187–1193.

MacDonald, C. J., Lepage, K. Q., Eden, U. T., and Eichenbaum, H. (2011). Hippocampal “time cells” bridge the gap in memory for discontiguous events. *Neuron*, 71(4):737–749.

Machado, A. (1997). Learning the temporal dynamics of behavior. *Psychological review*, 104(2):241.

Maricq, A. V. and Church, R. M. (1983). The differential effects of haloperidol and methamphetamine on time estimation in the rat. *Psychopharmacology*, 79(1):10–15.

Matell, M. S. and Meck, W. H. (2000). Neuropsychological mechanisms of interval timing behavior. *Bioessays*, 22(1):94–103.

Matell, M. S. and Meck, W. H. (2004). Cortico-striatal circuits and interval timing: coincidence detection of oscillatory processes. *Cognitive brain research*, 21(2):139–170.

Mauk, M. D. and Buonomano, D. V. (2004). The neural basis of temporal processing. *Annu. Rev. Neurosci.*, 27:307–340.

Meck, W. H. (2006). Neuroanatomical localization of an internal clock: a functional link between mesolimbic, nigrostriatal, and mesocortical dopaminergic systems. *Brain research*, 1109(1):93–107.

Meck, W. H. and Ivry, R. B. (2016). Editorial overview: Time in perception and action. *Current Opinion in Behavioral Sciences*, (8):vi–x.

Mello, G. B., Soares, S., and Paton, J. J. (2015). A scalable population code for time in the striatum. *Current Biology*, 25(9):1113–1122.

Merchant, H. (2014). *Neurobiology of Interval Timing*, volume 829.

Merchant, H., Harrington, D. L., and Meck, W. H. (2013). Neural basis of the perception and estimation of time. *Annual review of neuroscience*, 36:313–336.

Middleton, F. A. and Strick, P. L. (2000). Basal ganglia and cerebellar loops: motor and cognitive circuits. *Brain research reviews*, 31(2-3):236–250.

Mita, A., Mushiake, H., Shima, K., Matsuzaka, Y., and Tanji, J. (2009). Interval time coding by neurons in the presupplementary and supplementary motor areas. *Nature neuroscience*, 12(4):502.

Oorschot, D. E. (1996). Total number of neurons in the neostriatal, pallidal, subthalamic, and substantia nigral nuclei of the rat basal ganglia: a stereological study using the cavalieri and optical disector methods. *Journal of Comparative Neurology*, 366(4):580–599.

Pastalkova, E., Itskov, V., Amarasingham, A., and Buzsáki, G. (2008). Internally generated cell assembly sequences in the rat hippocampus. *Science*, 321(5894):1322–1327.

Paton, J. J. and Buonomano, D. V. (2018). The Neural Basis of Timing: Distributed Mechanisms for Diverse Functions. *Neuron*, 98(4):687–705.

Paxinos, G. and Watson, C. (2006). *The Rat Brain in Stereotaxic Coordinates: Hard Cover Edition*. Elsevier Science.

Payne, B. R., Lomber, S. G., Villa, A. E., and Bullier, J. (1996). Reversible deactivation of cerebral network components. *Trends in neurosciences*, 19(12):535–542.

Pires, A. and Hoy, R. R. (1992). Temperature coupling in cricket acoustic communication. *Journal of Comparative Physiology A*, 171(1):79–92.

Riffat, S. and Ma, X. (2003). Thermoelectrics: A Review of Present and Potential Applications. 23:913–935.

Robertson, R. M. and Money, T. G. (2012). Temperature and neuronal circuit function: compensation, tuning and tolerance. *Current opinion in neurobiology*, 22(4):724–734.

Schütt, H. H., Harmeling, S., Macke, J. H., and Wichmann, F. A. (2016). Painfree and accurate Bayesian estimation of psychometric functions for (potentially) overdispersed data. *Vision Research*, 122:105–123.

Smith, Y., Bennett, B., Bolam, J., Parent, A., and Sadikot, A. (1994). Synaptic relationships between dopaminergic afferents and cortical or thalamic input in the sensorimotor territory of the striatum in monkey. *Journal of Comparative Neurology*, 344(1):1–19.

Soofi, W., Goeritz, M. L., Kispersky, T. J., Prinz, A. A., Marder, E., and Stein, W. (2014). Phase maintenance in a rhythmic motor pattern during temperature changes in vivo. *Journal of neurophysiology*, 111(12):2603–2613.

Squire, L. R., Bloom, F. E., Spitzer, N. C., du Lac, S., Ghosh, A., and Berg, D. (2008). *Fundamental Neuroscience*.

Stephenson-Jones, M., Samuelsson, E., Ericsson, J., Robertson, B., and Grillner, S. (2011). Evolutionary conservation of the basal ganglia as a common vertebrate mechanism for action selection. *Current Biology*, 21(13):1081–1091.

Stoof, J. and Kebabian, J. (1981). Opposing roles for D-1 and D-2 dopamine receptors in efflux of cyclic AMP from rat neostriatum. *Nature*, 294:366–368.

Sze, S. M. and Ng, K. K. (2006). *Physics of semiconductor devices*. John wiley & sons.

Tang, L. S., Goeritz, M. L., Caplan, J. S., Taylor, A. L., Fisek, M., and Marder, E. (2010). Precise temperature compensation of phase in a rhythmic motor pattern. *PLoS biology*, 8(8):e1000469.

Tilley, R. J. (2004). *Understanding Solids: The Science of Materials*. John Wiley & Sons.

Ulrich, R. and Miller, J. (2004). Threshold estimation in two-alternative forced-choice (2afc) tasks: The spearman-kärber method. *Perception & Psychophysics*, 66(3):517–533.

Volgushev, M., Vidyasagar, T., Chistiakova, M., and Eysel, U. (2000a). Synaptic transmission in the neocortex during reversible cooling. *Neuroscience*, 98(1):9–22.

Volgushev, M., Vidyasagar, T. R., Chistiakova, M., Yousef, T., and Eysel, U. T. (2000b). Membrane properties and spike generation in rat visual cortical cells during reversible cooling. *The Journal of physiology*, 522(1):59–76.

Wernicke, C. (1874). *Der aphasische Symptomencomplex: eine psychologische Studie auf anatomischer Basis*. Cohn.

Wichmann, F. A. and Hill, N. J. (2001). The psychometric function: I.Fitting, sampling, and goodness of fit. *Perception & Psychophysics*, 63(8):1293–1313.

Wilson, C. J. and Groves, P. M. (1980). Fine structure and synaptic connections of the common spiny neuron of the rat neostriatum: a study employing intracellular injection of horseradish peroxidase. *Journal of Comparative Neurology*, 194(3):599–615.

Xu, M., Zhang, S.-y., Dan, Y., and Poo, M.-m. (2014). Representation of interval timing by temporally scalable firing patterns in rat prefrontal cortex. *Proceedings of the National Academy of Sciences*, 111(1):480–485.